Characterization and validation of 15 α-synuclein conformation-specific antibodies using well-characterized preparations of α-synuclein monomers, fibrils and oligomers with distinct structures and morphology: How specific are the conformation-specific α-synuclein antibodies?

Senthil T. Kumar[1#], Somanath Jagannath[1#], Cindy Francois[2], Hugo Vanderstichele[2], Erik Stoops[2] & Hilal A. Lashuel*[1]

[1] Laboratory of Molecular and Chemical Biology of Neurodegeneration, Brain Mind Institute, EPFL, Switzerland

[2] ADx NeuroSciences, Technologiepark 94, Ghent, Belgium.

Running title: Characterization of conformation-specific α-synuclein antibodies

* To whom correspondence should be addressed: Laboratory of Molecular and Chemical Biology of Neurodegeneration, Brain Mind Institute, Ecole Polytechnique Fédérale de Lausanne, 1015 Lausanne. Tel: +41216939691, Fax: +41216939665.
e-mail: hilal.lashuel@epfl.ch

# These authors contributed equally to the manuscript

Keywords: α-Synuclein, Parkinson's disease, Conformational antibodies, Oligomers, and Binding specificity

Abstract

Increasing evidence suggests that alpha-synuclein (α-syn) oligomers are obligate intermediates in the pathway involved in α-syn fibrillization and Lewy body (LB) formation, and may also accumulate within LBs in Parkinson's disease (PD) and other synucleinopathies. Therefore, the development of tools and methods to detect and quantify α-syn oligomers has become increasingly crucial for mechanistic studies to understand the role of these oligomers in PD, and to develop new diagnostic methods and therapies for PD and other synucleinopathies. The majority of these tools and methods rely primarily on the use of aggregation state-specific or conformation-specific antibodies. Given the impact of the data and knowledge generated using these antibodies on shaping the foundation and directions of α-syn and PD research, it is crucial that these antibodies are thoroughly characterized, and their specificity or ability to capture diverse α-syn species is tested and validated. Herein, we describe an antibody characterization and validation pipeline that allows a systematic investigation of the specificity of α-syn antibodies using well-defined and well-characterized preparations of various α-syn species, including monomers, fibrils, and different oligomer preparations that are characterized by distinct morphological, chemical and secondary structure properties. This pipeline was used to characterize 17 α-syn antibodies, 15 of which have been reported as conformation- or oligomer-specific antibodies, using an array of techniques, including immunoblot analysis (slot blot and Western blot), a digital ELISA assay using single molecule array technology and surface plasmon resonance. Our results show that i) none of the antibodies tested are specific for one particular type of α-syn species, including monomers, oligomers or fibrils; ii) all antibodies that were reported to be oligomer-specific also recognized fibrillar α-syn; and iii) a few antibodies showed high specificity for oligomers and fibrils but did not bind to monomers. These findings suggest that the majority of α-syn aggregate-specific antibodies do not differentiate between oligomers and fibrils, thus highlighting the importance of exercising caution when interpreting results obtained using these antibodies. Our results also underscore the critical importance of the characterization and validation of antibodies before their use in mechanistic studies and as diagnostic and therapeutic agents. This will not only improve the quality of research and reduce costs but will also reduce the number of therapeutic antibody failures in the clinic.

Introduction

Several neurodegenerative disorders are characterized by the presence of cytoplasmic proteinaceous inclusions termed Lewy bodies (LBs), which are enriched in misfolded and aggregated forms of the presynaptic protein alpha-synuclein (α-syn) (Goedert *et al.* 2017). These diseases include Parkinson's disease (PD), dementia with Lewy bodies (DLB), and multiple system atrophy (MSA), which are collectively referred to as synucleinopathies. Early studies of the ultrastructural properties and compositions of LBs revealed that they are highly enriched in filamentous structures (Duffy & Tennyson 1965; Lashuel 2020), which were later shown to be composed of α-syn (Spillantini *et al.* 1997; Spillantini *et al.* 1998). These findings, combined with the discovery that mutations in the gene that encodes α-syn causes early-onset forms of PD (Polymeropoulos *et al.* 1997), led to the hypothesis that the process of α-syn fibrillisation and LB formation plays a central role in the pathogenesis of PD and other synucleinopathies. However, the failure of this hypothesis to explain several neuropathological and experimental observations prompted the possibility that intermediates generated on the pathway to α-syn fibrillization and LB formation, rather than the fibrils or LBs themselves, are the primary toxicity-inducing and disease-causing species. These observations include 1) the lack of a strong correlation between Lewy pathology burden, neurodegeneration and disease severity (Colosimo *et al.* 2003; Parkkinen *et al.* 2008); 2) the presence of LBs in the brains of individuals who do not show any symptoms of PD or other synucleinopathies at the time of death (Parkkinen *et al.* 2005; Frigerio *et al.* 2011); and 3) the identification of patients who exhibit Parkinsonian symptoms in the absence of LBs e.g. PD patients harboring parkin and LRRK2 G2019S mutations (Kay *et al.* 2005; Gaig *et al.* 2006; Cookson *et al.* 2008; Johansen *et al.* 2018). These observations are similar to those demonstrating the lack of a correlation between amyloid-plaque burden and cognitive decline in Alzheimer's disease (AD) (Nelson *et al.* 2012; Jung *et al.* 2016; Arboleda-Velasquez *et al.* 2019), which have supported the toxic oligomer hypothesis of AD.

Several lines of evidence support the α-syn oligomer hypothesis. Both on- and off-pathway soluble and nonfibrillar α-syn oligomers of different sizes and morphologies were consistently observed during the *in vitro* aggregation of α-syn under different conditions (Conway *et al.* 2000; Lashuel *et al.* 2002; Cappai *et al.* 2005). Subsequent studies over the past decade have also provided evidence for the presence of α-syn oligomers in biological fluids such as saliva, blood plasma,

basal tears, and cerebrospinal fluid (CSF) from patients suffering from PD and other synucleinopathies (El-Agnaf *et al.* 2006; Tokuda *et al.* 2010; Hirohata *et al.* 2011; Wang *et al.* 2011; Majbour *et al.* 2016; Vivacqua *et al.* 2016; Hamm-Alvarez *et al.* 2019). Several of these studies suggested that the level of oligomers is correlated with the diagnosis of PD and disease progression (Sharon *et al.* 2003; El-Agnaf *et al.* 2006; Paleologou *et al.* 2009). One major caveat of these studies is that they were potentially carried out using tools and immunoassays that do not distinguish between oligomers and other higher-order aggregated forms of α-syn (fibrils or amorphous aggregates). Nonetheless, they paved the way for further studies demonstrating that α-syn oligomers/aggregates are secreted by neurons (Sharon *et al.* 2003; Tofaris *et al.* 2003; Jang *et al.* 2010; Tokuda *et al.* 2010; Majbour *et al.* 2016) in the brain, and could mediate the propagation of α-syn pathology and cause neurodegeneration. Indeed, several studies have shown that α-syn oligomers are released by neurons via exocytosis (Jang *et al.* 2010) and are then taken up by other cells via different mechanisms, including endocytosis (Desplats *et al.* 2009), trans-synaptic propagation (Danzer *et al.* 2012) or receptor-mediated uptake (Lee *et al.* 2008). Furthermore, α-syn oligomers have been shown to directly or indirectly contribute to α-syn-induced toxicity and neurodegeneration via different mechanisms, including but not limited to i) the disruption of cell membrane integrity by the formation of pores in the membrane (Volles *et al.* 2001; Danzer *et al.* 2007); ii) synaptic toxicity or neuronal signaling dysfunction (Diógenes *et al.* 2012; Rockenstein *et al.* 2014; Kaufmann *et al.* 2016; van Diggelen *et al.* 2019); iii) the failure of protein degradation pathways (Cuervo *et al.* 2004; Klucken *et al.* 2012; Tekirdag & Cuervo 2018); iv) endoplasmic reticulum dysfunction (Colla *et al.* 2012); v) mitochondrial dysfunction (Parihar *et al.* 2009; Di Maio *et al.* 2016); and vi) the enhancement of inflammatory responses (Wilms *et al.* 2009). These observations, combined with the overwhelming evidence that oligomer-induced toxicity is a key contributor or driving force leading to neurodegeneration in Alzheimer's disease (AD), fueled greater interest in the development of tools, therapies and diagnostics that specifically target α-syn oligomers. This includes the development of various protocols for the preparation of oligomers, the generation of oligomer-specific antibodies to target and clear oligomers, and immunoassays for quantifying oligomers.

Oligomers can be broadly defined as all the soluble oligomeric species that exist before the formation of α-syn fibrils, including a) dimers, trimers and low molecular weight assemblies,

which are not easily discernable by electron microscopy (EM) and atomic force microscopy (AFM)), and b) higher molecular weight oligomers with different morphologies that are composed of >10 monomers, which are easily detectable by EM, AFM and other imaging techniques (Lashuel *et al.* 2002; Lashuel & Lansbury 2006; Stöckl *et al.* 2013; Cremades *et al.* 2017; Ruggeri *et al.* 2018; Kumar *et al.* 2020). Our current knowledge of the biophysical properties of α-syn oligomers has been shaped primarily by results obtained by investigating α-syn aggregation and fibril formation *in vitro*. The propensity of α-syn to form oligomers is highly dependent on several factors, such as the protein concentration and sequence (including the presence of disease-associated mutations and post-translational modifications) (Lashuel *et al.* 2002; Paslawski *et al.* 2014a; Paslawski *et al.* 2014b), interactions with metals, other proteins and small molecules, and chemical modification by specific molecules (e.g. dopamine, 4-oxo-2-nonenal, 4-hydroxy-2-nonenal (HNE), and epigallocatechin gallate) (Danzer *et al.* 2007; Qin *et al.* 2007; Ehrnhoefer *et al.* 2008; Näsström *et al.* 2011b). Depending on the studied conditions, different types of α-syn oligomers have been consistently observed *in vitro*, and include globular, spherical, amorphous and pore-like oligomers (Figure 1) (Lashuel *et al.* 2002; Kumar *et al.* 2020). It remains unknown to what extent these oligomers resemble the oligomers that form in different cell types in the brains of patients. Several studies have reported the detection of oligomers in cell cultures, in the brains of animal models of synucleinopathies, and during the analysis of cerebrospinal fluids (CSF) and postmortem examinations of brains of PD, DLB and MSA patients (Sharon *et al.* 2003; Tofaris *et al.* 2003; Jang *et al.* 2010; Tokuda *et al.* 2010; Majbour *et al.* 2016). However, the evidence to support the presence of specific oligomers in these studies has been based for the most part on the detection of SDS-resistant oligomeric bands by Western blotting (Baba *et al.* 1998; Sharon *et al.* 2003; Tsigelny *et al.* 2008), the use of proximity ligation assays (Roberts *et al.* 2015), or the reliance on "oligomer-specific" antibodies or immunoassays. Thus, much of the knowledge and many of the hypotheses in the field today are based on conclusions drawn from studies relying on antibodies.

One major untested assumption related to the use of oligomer-specific antibodies and immunoassays is that the antibodies used are capable of capturing the structural and morphological diversity of α-syn oligomers *in vivo*. Notably, all of these antibodies were generated using specific recombinant α-syn aggregates, fibrils or oligomers generated under *in vitro* conditions. Some of

the limitations of existing antibody validation approaches include the following: 1) the lack of detailed characterization of *in vitro* oligomer preparations with respect to their purity, homogeneity and structural properties; 2) the use of oligomer preparations that may not reflect the conformational, biochemical and morphological diversity that exists in the brain; and 3) the lack of research that establishes whether specificity is driven by high affinity for oligomers, or by the avidity binding characteristics of antibodies.

Given the impact of the use of antibodies on shaping our knowledge of α-syn and its role in health and disease, and on developing diagnostics and therapies for PD and synucleinopathies, we developed a protocol for the systematic assessment of the specificity of α-syn antibodies using well-defined and well-characterized preparations of α-syn fibrils, oligomers, and monomers. This approach was then used to evaluate a library of 17 α-syn antibodies, 15 of which were reported to be aggregate-specific (Table 2). These antibodies can be broadly classified depending on the immunogens used for their generation: oligomers based on the use of i) a modified version of full-length α-synuclein (antibody clones 24H6, 12C6, 26F1, and 26B10); ii) α-syn fibrils pre-formed *in vitro* (PFFs) (antibody clones 7015, 9029, SYNO2, SYNO3, and SYNO4); iii) recombinant α-syn aggregates (antibody clones A17183A, A171183B, A17183E, and A17183G); iv) synthetic α-syn peptides encompassing amino acids 44 to 57 (5G4) or amino acid 1 to the C-terminus filament (MJFR-14); vi) recombinant full-length α-syn monomers (SYN211); and vi) a recombinant truncated α-syn variant consisting of residues 15-123 (SYN-1) (Table 2). To verify the specificity of these antibodies, we first screened them all against well-characterized preparations of α-syn species (monomers, oligomers, and fibrils) using immunoblot analysis (slot blotting and Western blotting) and a digital enzyme-linked immunosorbent assay (ELISA) using single molecule array (SIMOA) technology (Figure 1). To further scrutinize the conformational specificity of the antibodies, we tested them against different preparations of oligomers, which were characterized according to their distinct morphological, chemical and secondary structure properties. Finally, the binding affinity of selected antibodies was determined using surface plasmon resonance (SPR). This approach enabled us to define the specificity of the antibodies to a high degree and show that although some antibodies were specific for aggregated forms of α-syn and did not recognize monomers, all antibodies that were reported to be oligomer-specific also recognized fibrillar α-syn. Furthermore, some of the antibodies that were reported to be oligomer- or fibril-specific also

recognized α-syn monomers. We also identified an antibody that showed a preference for β-sheet-enriched fibrils and oligomers, but not for disordered oligomers or monomers. Our studies reveal that none of the antibodies showed any unique preferential specificity for one particular form of α-syn species, including monomers, oligomers or fibrils, andthat it is possible to develop antibodies that recognize diverse α-syn oligomers and fibrils. Our work underscores the importance of using well-characterized tools (*in vitro*-produced calibrants) and multiple methods to define the specificity of antibodies. This will not only help us to advance PD research, but will also improve the selection of promising antibody candidates and reduce the number of failures in advanced clinical trials of PD therapeutics.

Results

Preparation and characterization of α-syn monomers, unmodified oligomers and fibrils

To investigate the specificity of the antibodies listed in Table 2, we first assessed their specificity towards α-syn monomers, oligomers, and fibrils. To accomplish this goal, we generated well-characterized preparations of human 1) α-syn fibrils, 2) unmodified oligomers and 3) monomers that were free of cross-species contamination. The purity of each preparation was verified using our recently described centrifugation-filtration protocol (Kumar *et al.* 2020) (Figure 2A). Given that α-syn oligomers and fibrils are always in equilibrium with monomers, it is difficult to eliminate the presence of monomers completely. To minimize the number of monomers, all fibril and oligomeric samples were immediately subjected to centrifugation-filtration protocol as previously described (Kumar *et al.* 2020). Under these conditions, such preparations normally contain 10-20% monomers. Similarly, to ensure that the α-syn monomeric preparations were free of any preformed aggregates, the monomeric samples were filtered through a 100 kDa filter, and the flow-through (aggregate-free monomers) was collected and kept on ice and used immediately.

Several protocols have been developed to produce a homogenous population of oligomers *in vitro*, but all result in preparations that contain mixtures of oligomers that are structurally and morphologically diverse. However, it is possible to generate preparations that are enriched in specific oligomeric species (Lashuel *et al.* 2002; Lashuel & Lansbury 2006). The protocols involve the generation of oligomers either by incubating recombinant α-syn monomers at high

concentrations in buffers with or without additional components such as dopamine (Conway *et al.* 2001; Cappai *et al.* 2005; Norris *et al.* 2005; Leong *et al.* 2009; Rekas *et al.* 2010; Volpicelli-Daley *et al.* 2011; Choi *et al.* 2013; Planchard *et al.* 2014), lipids (Broersen *et al.* 2006; Trostchansky *et al.* 2006; Qin *et al.* 2007; Nasstrom *et al.* 2009; Näsström *et al.* 2011a; Näsström *et al.* 2011b; De Franceschi *et al.* 2011; Diógenes *et al.* 2012; Xiang *et al.* 2013), metals (Lowe *et al.* 2004; Cole *et al.* 2005; Danzer *et al.* 2007; Danzer *et al.* 2009; Wright *et al.* 2009; Schmidt *et al.* 2012), alcohols (Danzer *et al.* 2007; Danzer *et al.* 2009; Illes-Toth *et al.* 2015) (Ehrnhoefer *et al.* 2008), or by using methods that are based on the use of chemical cross-linking agents (Ruesink *et al.* 2019). In the absence of additional components, oligomers (hereafter referred to as unmodified oligomers) are found to exhibit heterogeneous morphologies, such as globular, spherical, annular pore-shaped, rectangular and tubular-shaped, and are usually but not always enriched in β-sheet structures (Lashuel *et al.* 2002). In the presence of additional components such as dopamine, lipids or alcohols, oligomers are found to have spherical, globular, rod-shaped or curvilinear morphologies, which are structurally different from primarily disordered, α-helical or β-sheeted structures, suggesting that the formation of oligomers is strongly influenced by the environment in which they form (Conway *et al.* 2001; Lowe *et al.* 2004; Norris *et al.* 2005; Broersen *et al.* 2006; Danzer *et al.* 2007; Nasstrom *et al.* 2009; Rekas *et al.* 2010; De Franceschi *et al.* 2011; Näsström *et al.* 2011a; Diógenes *et al.* 2012; Bae *et al.* 2013; Choi *et al.* 2013; Fecchio *et al.* 2013; Planchard *et al.* 2014).

Recombinant α-syn was used for the preparation of unmodified oligomers and fibrils. For the preparation of oligomers (Lashuel *et al.* 2002; Paslawski *et al.* 2016), 12 mg/mL α-syn monomer was dissolved in PBS and incubated at 37°C and 900 rpm for 5 h. After incubation, the sample was centrifuged, and the supernatant was applied to a size exclusion chromatography (SEC) column (Hiload 26/600 Superdex 200 pg) to separate the monomers from the oligomers (Figure 2B). Analysis of these fractions by SDS-PAGE under denaturing conditions showed the expected profile of monomeric and high molecular weight (HMW) bands, suggesting that the oligomer preparations contained a mixture of SDS-resistant and SDS-sensitive oligomers. An alternative explanation could be that the observed monomers were released from the ends/surfaces of the oligomers in the presence of SDS, whereas the core of the oligomers was stable and SDS-resistant. The HMW species (with a molecular weight distribution of up to 1 MDa) could be visualized at the top of the resolving portion of the gel (Figure 2C). As expected, the monomers that were

separated using SEC, it appeard in the gel around 15 kDa (Figure 2D), which was consistent with the expected MW of α-syn of 14461 Da (Figure 2E). The samples were analyzed by CD spectroscopy to ensure that each of the preparations exhibited the expected secondary structure signatures of oligomers and monomers. Oligomers exhibited a CD spectrum with a broad minimum peak centered at 219 nm, indicating the presence of mixed secondary structure contents dominated by β-sheet structures (Figure 2F). Monomers possessed a peak with the minimum at 198 nm consistent with their predominantly disordered structures (Figure 2F).

Next, we performed EM studies on monomers and oligomers. Because of their small size (~14 kDa), the monomers are not visible by electron microscopy (Figure 2G). In contrast, the EM of the oligomer preparations showed heterogeneous morphologies consisting of annular pores and spherical and rectangular tubular-like shaped particles (Figure 2H) (Lashuel *et al.* 2002) with a mean width of approximately 10 nm (Figure 2I). To prepare the fibrils, we followed the protocol described in Kumar et al., 2020; Mahul-Mellier et al., 2020. In brief, the lyophilized monomers (~300 μM) were dissolved in PBS and incubated shaking at 37 °C for five days at 1000 rpm. Next, we used our filtration protocol (Kumar *et al.* 2020) to remove any remaining monomers and oligomers from the fibril preparations. The fibrils are enriched in β-sheet structures, as evidenced by the minimum peak at 221 nm in the CD spectrum shown in Figure 2J and the characteristic streaking pattern in the SDS-PAGE analysis, which confirmed the presence of SDS-resistant high molecular weight species of α-syn (Figure 2K). Ultrastructural analysis revealed that these fibrils were polymorphic with fibril morphologies including straight, twisted, or stacked structures (Figure 2L), with a mean width of approximately 13 nm (Figure 2M).

Stability of α-syn preparations

Since these preparations were to be characterized in different labs, we investigated their stability to ensure that they would not change their properties due to the shipping and storage conditions. Therefore, we subjected the oligomers to several cycles of freezing and thawing by snap-freezing them 3-4 times followed by room temperature thawing and incubation at temperatures of 4°C and 37°C for 2 days, and then we determined whether they underwent any morphological changes by electron microscopy (Figure 2N). Interestingly, we found that the morphological distribution of

the oligomers was not significantly altered when the oligomers were subjected to up to 3-4 freeze-thaw cycles or incubated at 4°C for 2 days (Figure 2O and 2I). However, the oligomeric mean width was slightly reduced by approximately 6% after incubation at 37°C (Figure 2O), which could be due to the release of α-syn monomers from the oligomeric structures.

We also tested the stability of the unmodified oligomers using the digital ELISA assay based on the differences in the level of detection of oligomers at known concentrations under different solution conditions. Unmodified oligomers at two concentrations (20 and 200 pg/mL) were incubated at three different temperatures (+2 to 8°C, +20 to 25°C and +36 to 38°C) for different durations (2, 4 and 24 h). In parallel, the effect of freezing and thawing (F/T) the samples 1x, 3x, and 5x was also tested. These samples were analyzed by the SIMOA sandwich assay using the A17183B antibody, which was captured on beads.

As shown in Figure 2P and 2Q, our data indicated that a minor part of stability issues of oligomeric α-syn can be due to the effect of time and temperature, particularly at 4°C and 22°C. At an elevated temperature (37°C) in combination with long incubation time (24 h), there was a decrease in the signal. We noticed a decrease in the signal of the oligomers that underwent freeze/thaw cycles at lower concentrations (20 pg/mL) but not at higher concentrations (100 pg/mL). This evaluation did not include any optimization regarding the formulation of the oligomeric α-synuclein to ensure optimal stability in the follow-up experiments shown in Figure 4. However, these data, as well as the results of the EM analysis did not indicate any significant changes in the stability of the unmodified oligomers.

Profiling the reactivity of antibodies to different α-syn species by immunoblotting

To assess the specificity of the antibodies, we first performed slot blot analysis to assess the cross-reactivity of the antibodies listed in Table 2 toward α-syn monomers, unmodified oligomers, and fibrils. The use of slot blotting allowed us to assess the immunoreactivity and specificity of these antibodies towards the native conformations of three α-syn species (Figure 3A). Among the 17 antibodies tested, 15 were reported in the literature to be conformation-specific; see Table 2 (Kovacs *et al.* 2012; Vaikath *et al.* 2015; Covell *et al.* 2017; van Diggelen *et al.* 2019). The

remaining two antibodies, Syn 211 (which recognizes an epitope in the C-terminus region spanning residues 121-125) (Giasson *et al.* 2000) and SYN-1 (which recognizes an epitope in the NAC region spanning residues 91-99 of α-syn) (Perrin *et al.* 2003), are sequence-specific and recognized all three species. Surprisingly, we found that none of the antibodies tested in our study had specific reactivity towards only one particular species of α-syn (either the monomer, unmodified oligomers or fibrils). All 15 antibodies detected both unmodified oligomers and fibrils. Interestingly, among these, 1) the antibody clone 5G4 showed exceptional reactivity towards unmodified oligomers and fibrils in a concentration-dependent manner (increased dose dependency) and almost no reactivity towards monomers at both concentrations tested; 2) the antibodies SYNO3 and A17183E showed stronger reactivity towards unmodified oligomers and fibrils but very weak (only at high concentrations) or no reactivity towards monomers. Except for these two antibodies, the rest of the antibodies fell into one of the following three categories: i) antibodies that recognized unmodified oligomers and fibrils (even at low concentrations) with higher specificity than monomers (clones 26F1, SYNO2, and A17183B; ii) antibodies that recognized oligomers and fibrils in a concentration-dependent manner (high concentration → stronger detection) but also showed weak reactivity towards monomers at high concentrations (clones 24H6, A17183A, SYNO4, 7015, 26B10, and A17183G); and 3) antibodies that were non-specific and recognized all three forms of α-syn (clones 9029, 12C6, and MJFR-14) (Figure 3A; summarized in Table 5).

Given that many of these antibodies are also commonly used to assess the presence or formation of α-syn aggregates in cellular and animal models of synucleinopathies and brain tissues using Western blotting, we assessed their reactivity toward α-syn monomers, unmodified oligomers, and fibrils under complete or partial denaturing conditions. As expected, the sequence-specific antibodies SYN211 and SYN-1 showed stronger reactivity towards monomers, oligomers and high molecular weight fibrils (Giasson *et al.* 2000; Perrin *et al.* 2003). This is consistent with the fact that the epitopes of these antibodies are outside of the domains that form the cores of oligomers and fibrils. Interestingly, the antibodies 5G4 and A17183A showed no reactivity towards any of the three α-syn species under denaturing conditions, confirming their conformational specificity. The 24H6 antibody weakly reacted with the oligomeric band (at the top of the resolving gel) but not the band corresponding to monomeric α-syn or the HMW bands of the fibrillar samples. This

suggests that this antibody is specific for SDS-resistant oligomers; this is consistent with the detection of oligomers in the slot blot analysis (Figure 3B).

The rest of the antibodies reacted with the oligomeric and high molecular weight bands in fibrils, although the antibody clones A17183E and 26F1 weakly detected monomers. This was consistent with the weak monomer detection observed in the slot blots. In contrast, several antibodies, including SYNO3, A17183B, 26B10, 9029, 12C6, MJFR-14, 7015 and SYNO4, which were reported to be oligomer/aggregate-specific, showed cross-reactivity and detected SDS-denatured monomers, SDS-resistant oligomers and high molecular weight bands in fibrillar samples without any preference for one form of α-syn. These results highlight the critical importance of using the appropriate antibodies to detect and quantify α-syn species in biological samples from cellular and animal models of synucleinopathies.

However, some antibodies showed discrepancies: i) the antibody clone A17183G did not detect any 15 kDa band in the monomeric and oligomeric samples but was able to detect monomeric and dimeric bands in the fibril samples; ii) the antibody clone SYNO2 detected oligomeric bands in oligomer samples and dimeric bands in fibril samples but hardly detected monomeric bands, which was consistent with the slot blot findings for this antibody. Taken together, these results suggest that all the antibodies tested here do not preferentially detect one particular α-syn species (as confirmed by the slot blot analysis). Furthermore, WB analysis showed that many antibodies detected α-syn bands under denaturing conditions, which raises questions about their conformational specificity (summarized in Table 5).

Next, we assessed the antibody specificity towards α-syn monomers, unmodified oligomers and fibrils using a sandwich ELISA assay. We employed this assay for the detection of antibody specificity against low picogram concentrations of α-syn species under soluble conditions. The assay format utilizes the covalent capture of conformation-specific antibodies by a microsphere. The three α-syn species described above were used as analytes at two concentrations (100 and 1000 pg/mL). A pan-synuclein antibody was included as a pairing antibody with the oligomer-specific antibody.

When monomeric α-syn was used as the analyte, 12 of the 15 antibodies yielded signal-to-noise (S/N) values lower than the two values that were used as thresholds (Figure 4A). Three antibodies (clones 12C6, 7015 and 9029) showed S/N values higher than 2. When using fibrillar α-syn as an analyte, 14 antibodies resulted in S/N values higher than 2, while 26F1 showed reactivity in the presence of high concentrations (1000 pg/mL) but had lower than borderline reactivity toward 100 pg/mL of fibrils (Figure 4C). In terms of reactivity against oligomeric α-syn, 14 antibodies yielded S/N values higher than 2, although four antibodies (A17183E, 26F1, 24H6, and 26B10) possessed S/N values close to 2 in the presence of low concentrations of oligomers (100 pg/mL), but the reactivity was enhanced at high concentrations (1000 pg/mL). The antibody 5G4 yielded the lowest S/N value of 1 at both concentrations (Figure 4B).

The experiments revealed that several antibodies reacted with monomeric α-syn, including 12C6, 7015 and 9029, indicating their reduced specificity, whereas 7015 was borderline reactive. Those antibodies with strong reactivity toward oligomers (10 antibodies: A173183A, A173183B, A173183G, SYNO2, SYNO3, SYNO4, 12C6, 7015, 9029 and MJFR14) also had strong reactivity toward fibrils. The antibody 26F1 showed concentration-dependent reactivity toward oligomers and fibrils (high concentration → stronger reactivity), while the antibodies A17183E, 24H6, 26B10 and 5G4 showed greater fibril specificity. No antibodies could be identified that were solely oligomer-specific with no reactivity toward α-synuclein monomers or fibrils, as observed by the slot blot analysis (Figure 3A) (summarized in Table 5).

Characterization of the specificity of the antibodies toward morphologically and structurally different forms of oligomeric α-syn

Since our knowledge of the morphological and conformational properties of native oligomers in PD patient brains is unknown, we sought to further assess the specificity of the antibodies toward different preparations of oligomers that were structurally and morphologically different from the unmodified oligomers. The use of these different oligomer preparations allowed us to test whether differences in the morphologies/structures of α-syn oligomers could influence the reactivity or binding specificities of the antibodies, especially those that showed specificity toward oligomeric and/or aggregated forms of α-syn. We employed dopamine (DA) (Figure 5A) and 4-hydroxy-2-nonenal (HNE) (Figure 5B) to prepare cross-linked human WT α-syn oligomers. Several studies

have shown that the interaction of DA with α-syn promotes the formation of α-syn oligomers and influences α-syn aggregation propensity and neurotoxicity (Conway *et al.* 2001; Volpicelli-Daley *et al.* 2011; Mor *et al.* 2017), raising the possibility of the presence of DA-modified α-syn oligomeric species in PD patient brains. Similarly, HNE, a physiological byproduct of lipid peroxidation, has been shown to play roles in oxidative stress responses and alter the aggregation of α-syn in PD (Qin *et al.* 2007; Ingelsson 2016).

The DA- and HNE-α-syn oligomers (Figure 5 C and D) were prepared by the incubation of DA or HNE with α-syn, followed by the isolation of the oligomers using SEC as described in the previous section on the preparation of unmodified oligomers. The DA-induced oligomers exhibited CD spectra with a minimum at 198 nm, revealing the presence of species with predominantly disordered conformations and little structure (Figure 5 E, Table 4). However, the HNE-induced oligomers showed a broad CD spectrum centered at 219 nm that is more similar to the CD spectrum of unmodified oligomers, indicating the presence of β-sheet-enriched oligomers (Figure 5J, Table 4). Analysis of these fractions by SDS-PAGE analysis under denaturing conditions (Figure 5F: DA oligomers, Figure 4K: HNE oligomers) showed a very similar gel profile for both types of oligomers, with the presence of HMW bands at the top of the resolving part of the gel and a thin band of monomers at 15 kDa that may have been released from the oligomers.

EM ultrastructural analysis of the DA-induced oligomers showed the presence of oligomers with near-spherical morphologies and different shapes and sizes (Figure 5G), as previously shown (Conway *et al.* 2001; Cappai *et al.* 2005; Mahul-Mellier *et al.* 2015), and these oligomers had a mean width of approximately 13 nm (Figure 4I). However, the HNE-induced oligomers appeared to be more homogenous with curvilinear (chain-like) morphologies and to have a mean width of approximately 8 nm (Figure 5L and 5-N).

Next, we tested the stability of these oligomers with respect to changes in their sizes and oligomeric morphologies as described above for the oligomers shown in Figure 2. While the incubation conditions of the DA oligomers in freeze-thaw conditions and at 4 °C did not result in major differences in terms of the morphologies, the number/density of the oligomeric particles on the EM grids was significantly reduced for the DA oligomeric sample incubated at 37 °C (Figure 5H),

and a decrease in the mean width to approximately 10 nm was also observed (Figure 5I). However, the HNE oligomers, under identical conditions, did not show major changes in their morphologies and mean width (Figure 5M and 5N). This highlights the importance of the careful characterization of α-syn samples before utilizing them for any specific experiment and emphasizes the need for maintaining stable working conditions when handling the different types of oligomers.

To investigate whether the antibodies in Table 2 show differential reactivity to morphologically, chemically and conformationally distinct oligomer preparations under native conditions, we performed slot blot analysis of the reactivity of these antibodies toward DA- and HNE-induced oligomers and monomers as a control (Figure 6A). The majority of the antibodies we tested detected DA- and HNE-induced oligomers and monomers irrespective of their morphological or structural differences. Strikingly, among all the antibodies tested, 26F1 showed no reactivity toward DA-induced oligomers, weak reactivity toward monomers but very strong reactivity toward HNE-induced oligomers, which is consistent with the data shown in Figure 3A. 26F1 was generated against oligomerized HNE-modified α-syn. The 5G4 antibody, which does not recognize α-syn monomers, also showed strong reactivity toward HNE-induced oligomers but exhibited weak reactivity toward DA-induced oligomers, possibly suggesting the presence of a small population of DA oligomers with a hidden conformation, as was predicted by CD spectra deconvolution analysis (Table 4). As expected, the sequence-specific antibodies SYN211 and SYN-1 detected both DA- and HNE-induced oligomers and monomers.

The antibodies that showed stronger reactivity toward HNE-induced oligomers can be categorized further depending on their reactivity toward DA-induced oligomers and monomers as follows: i) A17183E showed enhanced detection of DA- and HNE-induced oligomers compared to monomers; ii) 24H6, A17183A, 26B10 and A17183G showed stronger reactivity to HNE-induced oligomers (even at a low concentration of protein of 36 ng per spot) and concentration-dependent detection of DA-induced oligomers and monomers; iii) SYNO2, SYNO3, SYNO4, A17183B, 7015 and 9029 showed enhanced detection of HNE- and DA-induced oligomers and concentration-dependent reactivity toward monomers (weak binding at a low concentration of monomers, 36 ng of protein per spot). In contrast, there were some antibodies, such as 12C6 and MJFR-14, that showed very strong nonspecific detection of DA- and HNE-induced oligomers as

well as monomers irrespective of the concentration of proteins loaded in each spot in the slot blot analysis.

In summary, our immunoblotting studies (Figure 3 and Figure 6) demonstrate that none of the antibodies showed any preferential specificity toward one particular α-syn species, including monomers, oligomers and fibrils. However, we observed some exceptions: i) the antibody clone 26F1 did not show any reactivity toward the largely unstructured DA-induced oligomers but was highly specific for β-sheet-enriched unmodified oligomers, HNE-induced oligomers and fibrils; ii) the antibody 5G4 showed weak reactivity toward the largely unstructured DA-induced oligomers but stronger reactivity towards β-sheet-enriched unmodified oligomers, HNE-induced oligomers and fibrils (summarized in Table 5). These differences in reactivity emphasize the importance of using many antibodies in parallel rather than a single antibody for the identification of pathological oligomers in the brain given the heterogeneous nature and structural properties of such oligomers.

Kinetics of the binding of α-syn monomers and unmodified oligomers to immobilized antibodies

To further characterize and validate the specificity of the antibodies, we assessed their binding affinity and kinetics to monomeric and oligomeric α-syn species using SPR (Figure 7A), which allows the monitoring of binding events between antibodies and α-syn species under native conditions. We immobilized the antibodies on the chip surface at low densities instead of oligomers or monomers to ensure the measurement of the binding affinity but not the avidity.

Figure 7 and SI Figure 1 show the SPR sensorgrams of selected immobilized antibodies (eight in total; seven conformational and one sequence-specific) as a function of time as obtained by the successive injection of monomers or oligomers at concentrations ranging from 30 to 2000 nM. Sensorgram plots were fitted to extract the kinetic parameters, such as the binding affinity (KD) and association (k_a) and dissociation (k_d) rate constants of the binding between antibodies and monomer or oligomer complexes. The fitting of the plots was based on either a 1:1 binding model, which provides kinetic data for one binding site or on a global heterogeneous ligand binding model,

which provides kinetic parameters for two binding sites. Collectively, all of the tested antibodies showed binding responses to both α-syn monomers and unmodified oligomers with varying binding affinities. Interestingly, many of the antibodies that were found to be highly specific for oligomers/fibrils (Figure 3A) also showed binding to monomers. However, the binding affinities (KD) of the antibodies A17183A, SYNO4, and 26F1 reflected μM affinities toward monomers, which was consistent with the slot blot data showing their weak reactivity toward monomers (Figure 3A). The kinetic parameters obtained from the sensorgrams are summarized in Table 3.

The shape of the dissociation portion of the SPR sensorgrams (after 120 seconds) provides clues about the binding affinity of the antibodies toward monomers or oligomers; a stronger affinity is reflected by a flatter slope of the dissociation curve (slower off-rate), but a weaker affinity is reflected by a steeper curve (faster off-rate). Figure 7 and Supplementary Figure 1 show the SPR sensorgrams of the antibodies in the presence of monomers and oligomers. Fitting with a 1:1 binding model was possible for the binding of a few antibodies (A17183A, SYNO4 and 26F1) to α-syn monomers, which showed a weak binding affinity (KD) toward α-syn monomers with a KD of 3.61 μM (A17183A), 5.67 μM (SYNO4) and 76 μM (26F1). However, the same antibodies, when fitted according to the heterogeneous binding model, showed the highest binding affinity for one of the two binding sites of the unmodified oligomers; these antibodies included A17183A (KD1: 3.67 μM, KD2: 45 nM), SYNO4 (KD1: 249 nM, KD2: 2.14 pM) and 26F1 (KD1: 2.12 μM, KD2: 279 pM) (Figure 7B and SI Figure 1A, Table 3). The weaker binding affinity for α-syn monomers but stronger affinity for oligomers was shown by the antibodies A17183A, SYNO4 and 26F1 is in agreement with our slot blot and Western blot analyses (Figure 3), confirming that these antibodies bind with greater specificity to oligomers than monomers.

In contrast, antibodies such as 12C6, MJFR-14 and 9029 showed similar and stronger binding affinities toward both monomers and oligomers (Figure 7C and SI figure 1B, Table 3), which is consistent with our slot blot analysis (Figure 3A), which revealed that these antibodies showed stronger reactivity toward monomers. The antibodies 12C6 and 9029 but not MJFR-14 showed binding to monomers based on ELISA (Figure 4A), even at picogram concentrations. In addition, as shown in Figure 3B), these antibodies detected α-syn, even though they were expected to detect the protein under denaturing conditions, which raises questions about the claims regarding their

conformational specificity. The antibody 9029 showed stronger binding to both monomers and oligomers, but fitting was not possible for calculating the kinetic rate constants and binding affinities. The stronger binding of antibodies such as 12C6, MJFR-14 and 9029 to monomers was revealed when the dissociation portion of the sensorgrams (after 120 seconds) did not reach zero response units (RU, y-axis) and instead showed strong RU signals indicating the presence of complexes that was almost the same shape as that of sensorgrams showing antibodies binding to oligomers. However, this was not the case for the dissociation phase of the sensorgrams of the binding of A17183A, 26F1, and SYNO4 to monomers, where the RU returned to zero, revealing the weak binding to monomers. As expected, SYN211, which recognizes all three forms of α-syn, showed a stronger affinity for monomers (Figure 7D). However, heterogenous fitting was only possible for the monomers showing the highest binding affinities (KD1: 271 μM, KD2: 217 nM). The fitting of SYN211 binding to oligomers was not possible but indicated stronger binding to oligomers, as reflected by the shape of the curves. The binding specificity was consistent with our slot blot analysis (Figure 3), which showed that SYN211 more strongly detected β-sheet-enriched oligomers than unstructured monomers at lower concentrations. The details of the kinetic parameters and binding affinities of these conformational-specific antibodies would be useful for PD/α-syn research for selecting an appropriate antibody for future studies.

Discussion

Increasing evidence supports the hypothesis that different forms of α-syn aggregates (e.g. fibrils and oligomers) play an important role in the pathogenesis of PD. Testing this hypothesis requires the development of therapeutic drugs or antibodies that target the different species and assays that enable the accurate assessment of changes in their levels during disease progression and in response to therapies. Although there are several biochemical, structural and imaging-based approaches for the direct and indirect visualization and characterization of α-syn fibrils (Shahmoradian *et al.* 2019; Lashuel 2020), detection of nonfibrillar oligomeric α-syn in cells or postmortem brain tissues remains challenging. The existing methods and techniques, such as Western blotting and proximity ligation assays, provide indications of the presence of oligomers but not information about their size, conformation and/or morphology. The instability and low abundances of native oligomers make the isolation and characterization of their structural

properties using NMR and Cryo-EM very challenging. Due to these challenges, researchers in the field have resorted to the development of conformation- or aggregate-specific antibodies.

One of the major untested assumptions about conformation-specific antibodies is that they are claimed to be capable of specifically capturing the structural and morphological diversity of α-syn species *in vivo* or to target a specific α-syn entity. However, these assumptions are never experimentally tested. Thus, the field requires the development of protocols for conducting systematic characterization of antibodies using a well-characterized and validated set of α-syn species. This would bring us closer to the goal of capturing the diversity of α-syn species involved in health and disease. To achieve this goal, we developed a protocol and evaluated the binding specificity of 17 antibodies that were procured from different sources (Table 2). First, the antibodies were screened against disordered monomers and β-sheet-enriched preparations of oligomers and fibrils. The first step enabled the identification of antibodies that were specific for oligomers or fibrils or both. To further assess whether antibody binding was indeed driven by conformational specificity or avidity, the antibodies were screened against three preparations of α-syn oligomers with distinct biochemical, conformational and morphological properties (disordered oligomers and oligomers with different β-sheet and secondary structure contents) (Table 4). Binding to these three distinct types of oligomers enabled us to determine whether the binding was driven by avidity or by the recognition of a specific conformation present in a unique aggregation state of the protein. In parallel, we also tested the reactivities and binding affinities of various α-syn antibodies by SIMOA assays and SPR, respectively. Evaluation using these approaches revealed the true nature of the conformational specificity of antibodies against α-syn aggregates.

None of the antibodies specifically detect either monomers, oligomers or fibrillar α-syn species

Surprisingly, we found that none of the antibodies tested in our study had unique specific reactivity toward one particular α-syn species (monomers, unmodified oligomers or fibrils). All 15 reported conformational-specific antibodies detected both unmodified β-sheet enriched oligomers and fibrils, demonstrating that they could not differentiate between oligomers and fibrils and are not specific for a particular conformation or α-syn aggregation state.

In an attempt to better capture the possible morphological and conformational diversity of native oligomers in the brain, we also produced oligomeric preparations (DA and HNE oligomers) possessing structurally and morphologically distinct properties (Figure 5). The immunoreactivity toward these oligomers was compared to that toward the oligomers prepared from unmodified α-syn, which are enriched in β-sheet structures (Figure 3 and Figure 6). Despite the similarity of the CD signatures of HNE-induced and unmodified α-syn oligomers, the two types of oligomers exhibited distinct morphological features (Figure 2 and Figure 5). The structural and morphological diversity of the different oligomer preparations provided a unique opportunity to assess the specificity of the conformational-specific antibodies.

The Syn 211 and SYN-1 antibodies detected all three α-syn species (monomers, oligomers and fibrils) as well as the DA- and HNE oligomers in both slot blots and Western blots owing to their sequence specificity (Figure 3) (Giasson *et al.* 2000; Perrin *et al.* 2003). This could be attributed to the fact that their epitopes are located in regions that do not constitute the core of α-syn oligomers or fibrils. This is supported by i) a previous study using hydrogen-deuterium exchange mass spectrometry to reveal that the core of oligomers consists of amino acid residues 39-89 and has N-and C-terminal regions that are highly exposed (Paslawski *et al.* 2014b); ii) the Cryo-EM structures of the α-syn rod and twister fibrils, which showed that these two types of fibrils share a conserved kernel consisting of a bent β-arch motif formed by residues 50-77 and residues 50-57 (preNAC region) and in which residues 66-78 (NACore region) form the interface of the two protofilaments in these fibrils (Li *et al.* 2018); iii) a subsequent cryo-EM study of full-length α-syn fibrils that reported the presence of two polymorphs that both conserved the kernel-shaped core with the additional presence of a β-strand formed by amino acids 16-23 outside of the common core region (Guerrero-Ferreira *et al.* 2019). Our results are consistent with previous studies in which Syn 211 was shown to detect monomers and HNE-induced oligomers (van Diggelen *et al.* 2019) and the detection of monomers and fibrils by SYN-1 (Vaikath *et al.* 2015; Weihofen *et al.* 2019) with dot blots. Interestingly, the antibody clone 5G4 showed increased reactivity with high conformational specificity for all forms of α-syn aggregates but showed very weak reactivity toward monomers. The surprising observation of the ability of 5G4 to bind DA oligomers (Figure 5) closer to the specificity as β-sheet enriched α-syn aggregates (Figure 3A and

5) suggests the presence of structures of minimal β-sheeted conformations (~11%) in DA oligomers (Table 4) that is recognized by 5G4. This is consistent with a previous study that reported that 5G4 detects widespread and distinct α-syn-induced pathology in the cortical and brain stem brain regions in postmortem synucleinopathic brain tissues, implying that this antibody detected different aggregated α-syn species (Kovacs *et al.* 2012). Consistent with our findings (Figure 3, Figure 5), Kovacs et al. 2012 also demonstrated that antibody clone 5G4 detects monomeric bands very faintly in brain homogenate samples from Lewy body dementia patients. Furthermore, van Diggelen et al. found that 5G4 antibody detected HNE-induced oligomers and showed no reactivity toward monomers (van Diggelen *et al.* 2019).

There are additional discrepancies between the findings of our study and previously published reports or data provided by the manufacturers. Previous reports indicated that the antibody MJFR-14 is a conformational-specific antibody and detects fibrillar and filamentous aggregates (Sampson *et al.* 2016; Elfarrash *et al.* 2019; Kawahata *et al.* 2019). However, here, we report that this antibody shows high reactivity toward well-characterized monomeric preparations, unmodified oligomers, and DA- and HNE-induced oligomers and fibrils, suggesting that this antibody is not a fibril-specific antibody. Similarly, Vaikath et al. reported that Syn O2, Syn O3, and Syn O4 can bind to α-syn oligomers and fibrils but not monomers (Vaikath *et al.* 2015). However, in our study, these antibodies (SYNO2 and SYNO3) did not show α-syn species specificity and detected α-syn monomers in a concentration-dependent manner (higher concentration of monomer → better reactivity). Recent findings by Covell et al. reported that the antibody clone 7015 a) detects LB and Lewy neurites (LNs) in all brain regions, b) detects LNs with increased specificity and Lewy dots colocalized with pS129, and c) does not show extensive colocalization of α-syn with ubiquitin and p62 (markers of late-stage α-syn pathology) (Covell *et al.* 2017). They also reported that Lewy dots are believed to appear early in the disease, implying that α-syn may preferentially bind to oligomers (precursors to fibrils). However, in our study, we found that this antibody does not distinguish between unmodified oligomers, DA- and HNE-induced oligomers and fibrils, although it showed relatively weak binding to monomers. This suggests that this antibody is not specific for oligomers or does not distinguish between α-syn aggregates. In the same study, Covell et al. also reported another antibody clone 9029, which detects Lewy pathology in all regions, detects fewer LNs than 7015, and colocalizes with the markers of late-stage α-syn pathology i.e. ubiquitin and

p62. In our study, we found that this antibody does not distinguish between monomers, different types of oligomers (unmodified oligomers and DA- and HNE-induced oligomers) or fibrils. This suggests that this antibody does not recognize particular α-syn species and is not a conformation-specific antibody.

Among the 17 antibodies in Table 2, the binding affinity and kinetics of only three antibodies (SYNO2, SYNO3, and SYNO4) against α-syn fibrils but not monomers or oligomers have been described in the literature or material provided by the manufacturer (Vaikath *et al.* 2015). Most importantly, we could not find any comparative SPR or binding studies using well-characterized preparations of α-syn monomers or different types of oligomers. By applying our filtration protocol to α-syn monomers or oligomers (Kumar *et al.* 2020), we ruled out the cross-contamination of α-syn species, verifying the SPR measurements of predominantly single α-syn species.

The comparison of the kinetics data and binding affinities of various antibodies for monomers and oligomers showed a significant degree of heterogeneity in the values of k_a, k_d, and KD (Table 3). The differences in the values of the dissociation rate constants (K_d) of most of the antibodies suggested that none of the antibodies showed binding specificity for a single epitope which could be common to α-syn monomers or oligomers. Antibody clones A17183A, 26F1, and SYNO4 showed high binding affinities for oligomers and weak binding affinities for monomers (Figure 7, Supplementary Figure 1 and Table 3). This suggests that these antibodies are highly conformationally specific for β-sheet-enriched oligomers compared to disordered monomers, which is in agreement with the slot blot and WB data (Figure 3A and B). Interestingly, the A17183A antibody showed stronger binding to unstructured DA oligomers (Figure 6), which may hint that the binding is, perhaps, driven by avidity rather than affinity. However, the 26F1 antibody showed specificity for β-sheet-enriched oligomers but not for unstructured DA oligomers, suggesting that it is truly conformationally specific. The ELISA analysis revealed that the antibody 26F1 showed differences in the level of reactivity based on the oligomer and fibril concentrations and showed increased reactivity at higher concentrations (1000 pg/mL= ~70 pM). This is expected, given the KD of 26F1 of 279 pM in the presence of oligomers. The very weak affinity of 26F1 with a KD of 76 μM for monomers is also in line with all our analyses, including the ELISA

analysis, suggesting that 26F1 is highly conformationally specific for β-sheet-enriched α-syn aggregates.

All the other antibodies, such as 12C6, 9029, and MJFR-14, showed stronger affinities for both monomers and oligomers (Figure 7, Supplementary Figure 1 and Table 4) and strong binding to DA oligomers, implying that these are unlikely to be conformational-specific and that their binding is mediated mostly by avidity towards α-syn oligomers. These results, match those of the ELISA assay, the antibodies 12C6, 7015, and 9029 had high reactivity towards monomers at low pg concentrations (Figure 4A; 100 and 1000 pg/mL concentration of monomers used). In fact, this is consistent with both the slot blot (~36 ng and ~180 ng of monomers spotted) and WB (~50 ng monomers loaded) analyses, where these antibodies showed high reactivity to monomers (Figure 3A) on slot blot and detected α-syn bands in denaturing Western blot analysis (Figure 3B). In addition, recent suggest that MJFR-14 is a conformation-specific with enhanced reactivity towards filaments but not to the denatured filaments or monomers (Martinez et al., 2016; Abcam (ab209538)). More specifically, i) data obtained using Luminex assay demonstrated an increased specificity of MJFR-14 antibody towards α-syn oligomers compared to monomers and filaments (Martinez et al., 2016) at low ng concentrations; ii) a study by Lassen et al. also reported that MJFR-14 is highly specific for oligomers but not to monomers (Lassen et al 2018). In line with these evidence, our ELISA Simoa assay showed that MJFR-14 does not bind to monomers at low picogram concentrations (Figure 4 A) but shows a better reactivity towards fibrils compared to oligomers (Figure 4B and C). In addition, our slot blot analysis (Figure 3A and Figure 6) showed stronger and similar reactivity towards oligomers and fibrils but a weaker reactivity to monomers at 36 ng concentrations. However, Western blot showed a similar detection pattern of α-syn bands of all α-syn species as comparable to sequence-specific antibodies such as SYN211 and SYN-1 antibodies (Figure 3B).

Limitations of our study:

One major limitation of our work is that while we used diverse and well-characterized α-syn preparations of monomers, oligomers (different types), and fibrils to screen the antibodies, it remains unclear to what extent these species occur in the brain. That being said, we hypothesized

that screening using a diverse set of species instead of using one specific type of α-syn oligomer is the best that we can do to approximate the complexity of α-syn species *in vivo*. The second limitation is that α-syn is subjected to different modifications *in vivo,* while all our protein standards were generated from unmodified recombinant α-syn. However, it is important to note that while we know a great deal about the different types of PTMs that occur in LBs and LNs and α-syn aggregates, very little is known about the PTM patterns of α-syn oligomers *in vivo*. Further studies are needed to address this knowledge gap. Finally, our studies focused on exploring the structural diversity of oligomers but not that of fibrils. We recognize this limitation and plan to address it in future studies.

Conclusions

Herein, we used multiple techniques to assess the α-syn species specificity of several commonly used conformational-specific antibodies. This was achieved by using well-characterized preparation of α-syn monomers, fibrils and different preparation of oligomers of distinct structural and biochemical properties. Our results demonstrated that i) no antibodies could be identified that were solely oligomer-specific, i.e. all the antibodies showed reactivity toward fibrillar and/or monomeric α-syn; ii) the antibody clone 26F1 is the only antibody that was shown to be highly specific for β-sheet-enriched oligomers, it detects unmodified oligomers and HNE-induced oligomers and fibrils but not for unstructured DA-induced oligomers and structurally disordered monomers; iii) the antibody clone 5G4 showed increased reactivity toward β-sheet-enriched unmodified oligomers, HNE-induced oligomers and fibrils, and unstructured DA-induced oligomers and almost no reactivity toward monomers; iv) antibodies clones A17183A, A17183E and SYNO4 preferentially detected all three types of oligomers and fibrils but reacted very weakly toward monomers; v) the majority of the other antibodies (such as 9029, 12C6, MJFR-14, SYN-1, and SYN211) exhibited reactivity towards all α-syn species under the conditions tested here. Although we failed to identify antibodies that target a single specific form of aSyn, i.e. monomers, oligomers or fibrils, our results show that it is possible to develop antibodies that target β-sheet rich α-syn oligomers and fibrils or oligomers and fibrils of diverse conformational properties. Such antibodies could represent more reliable tools for measuring the total levels of aggregated α-syn.

Finally, our findings show that it is unlikely that any of the existing oligomer-specific immunoassays are capable of providing an accurate assessment of the levels of α-syn oligomers. Therefore, we propose that these assays should be reassessed for their ability to distinguish between α-syn oligomers and fibrils and that interpretation of previous and future studies should take into account the specificity and limitation of the antibodies used. Future studies aimed at deciphering the role of different α-syn species in the pathogenesis of PD should be carried out using multiple antibodies that have been characterized using α-syn multiple calibrants that capture, to the extent possible, the diversity of α-syn species in the brain. A similar approach can be applied to facilitate the development of accurate assays to assess target engagement of therapeutic antibodies.

Authors' contributions

HV, ES and HAL conceived and conceptualised the study. STK, SJ, ES and HAL designed the experiments. STK and SJ performed all the experiments except ELISA. CF carried out the ELISA assay. STK, SJ, ES and HAL analysed the data. STK, SJ and HAL wrote the manuscript, with inputs from CF and ES.

Acknowledgments

We thank Dr. Ron Gill (senior scientist, Xsensio SA, Switzerland) for his critical review, helpful discussions and comments on the SPR data. We also thank the CIME facility (EPFL) for the use of their electron microscopy facility and Dr. Kelvin Lau from PTPSP (Protein Production and Structure Core Facility, EPFL) for their tremendous support and use of their SPR and CD instruments. We also thank Dr. Pedro Magalhães for his inputs with the details of α-syn concentration ranges in the body fluids. The authors also thank Guus Scheefhals (Syngle Therapeutics B.V.), Dr. Ramanath Hegde, Dr. Pedro Magalhães, Dr. Salvatore Novello, Firat Melek Altay and Ahmed Sadek (EPFL, Lausanne) for their critical review and feedback on the paper. We also thank Anass Chiki for providing the purified α-syn used for the preparation of DA- and HNE-induced oligomers, and Jonathan Ricci for his assistance with the initial setup of immunoblot studies. Antibodies with clones 7015 and 9029 were kindly provided by Dr. Kelvin

Luk, Prof. John Trojanowski and Prof. Virginia M. Lee (UPenn, USA). The generation of antibodies 24H6, 12C6, 26F1 and 26B10 was supported by a grant from the Michael J. Fox Foundation (DOSAB). This project was funded by the École Polytechnique Fédérale de Lausanne and the Michael J Fox Foundation.

Conflict of interest disclosure

Prof. Hilal A. Lashuel is the founder and chief scientific officer of ND BioSciences, Epalinges, Switzerland.

Materials and methods

Recombinant overexpression and purification of human WT α-syn

Recombinant overexpression and purification of human WT α-syn was performed as described previously (Fauvet *et al.* 2012) with slight modifications. pT7-7 plasmids encoding human WT α-syn were used for transformation in BL21 (DE3) *E-Coli* cells on an ampicillin agar plate. A single colony was transferred to 400 mL of Luria broth (LB) medium containing 100 µg/mL ampicillin (AppliChem, A0839) (small-scale culture) and incubated overnight at 37 °C and 180 rpm. On the next day, the pre-culture was used to inoculate 3-6 liters of LB medium having 100 µg/mL ampicillin (large-scale culture). Upon A_{600} approaching 0.4 to 0.6, α-syn protein expression was induced by the addition of 1 mM 1-thio-β-d-galactopyranoside (AppliChem, A1008) and the cells were further incubated at 37 °C and 180 rpm for four hours. This incubation step was followed by harvesting cells by centrifugation at 4000 rpm using JLA 8.1000 rotor (Beckman Coulter, Bear, CA) for 30 minutes at 5 °C. The harvested pellets were stored at -20 ºC until the next step. The cell lysis was performed by dissolving the bacterial pellet in buffer A (20 mM Tris–HCl, pH 7.5) containing protease inhibitors (1 mM EDTA (Sigma-Aldrich, 11873580001) and 1 mM PMSF (Applichem, A0999) followed by ultrasonication (VibraCell VCX130, Sonics, Newtown, CT) time: 5 min; cycle: 30 sec ON, 30 sec OFF; amplitude 70%. After lysis, centrifugation at 12000rpm and 4ºC for 30minutes was performed to collect the supernatant. This supernatant was collected in 50 mL Falcon tube and placed in boiling water (100 ºC) for about 15 minutes. This solution was subjected to another round of centrifugation at 12000 rpm and 4 ºC for 30 minutes. The supernatant

obtained at this step was filtered through 0.45 µm filters and injected into a sample loop connected to HiPrep Q FF 16/10 (GE healthcare, 28936543). The supernatant was injected at 2 mL/min and eluted using buffer B (20mM Tris-HCl, 1M NaCl, pH 7.5) from gradient 0 to 70% at 3 mL/min. All fractions were analyzed by SDS-PAGE, and the fractions containing pure α-syn were pooled and concentrated using a 30 kDa molecular weight cut-off (MWCO) filters (MERCK, UFC903008) at 4 ºC. The retentate was collected and dialyzed using 12-14 kDa MWCO Spectrapor dialysis membrane (Spectrum Labs, 9.206 67) against deionized water at 4 ºC overnight to remove salts. Dialyzed solution was collected, snap-frozen, and lyophilized.

Preparation of WT α-syn oligomers

To generate monomer and fibril free α-syn oligomeric preparations, 60 mg of lyophilized recombinant α-syn protein was dissolved in 5 mL PBS (10 mM disodium hydrogen phosphate, 2 mM potassium dihydrogen phosphate, 137 mM NaCl and 2.7 mM potassium chloride, pH 7.4) (final concentration: 12mg/mL) containing 5 µL Benzonase (final concentration: 1 µL benzonase/mL (MERCK, 71205-3). After dissolving, the solution is filtered through 0.22 µm filters (MERCK, SLGP033RS) and transferred to five low-protein binding 1.5 mL tubes, each containing 1 mL solution. These tubes were incubated in a shaking incubator at 37 ºC and 900 rpm for five hours. The samples were centrifuged at 12000*g* for 10 min at 4 ºC to remove any insoluble α-syn aggregates. 5 mL of supernatant was loaded into a sample loop of the chromatography setup. This sample was run through Hiload 26/600 Superdex 200pg (GE Healthcare, 28-9893-36) column equilibrated with PBS and eluted as 2.5 mL fractions at a flow rate of 1 mL/min. The elution of protein was monitored by UV absorbance at 280nm. Different fractions were visualized by SDS-PAGE analysis, and fractions of interest (oligomer) corresponding to the void volume peak were aliquoted (500 µL), snap-frozen, and stored at -20 ºC.

Preparation of DA-induced oligomers

DA-induced oligomers were prepared as described previously (Mahul-Mellier *et al.* 2015). Briefly, the recombinant α-syn protein was dissolved in 20mM Tris and 100mM NaCl to have a final concentration of 140 µM (pH 7.4). After dissolving, the protein solution was filtered through a 100 kDa filter (MERCK, MRCFOR100). The filtrate was transferred to a low-protein binding tube and 20 equivalents of dopamine (final concentration: 2.8 mM) (Sigma-Aldrich, H8502) was added.

This tube was covered with aluminum foil and incubated in a shaking incubator at 37 ºC and 200 rpm for five days. The sample was centrifuged at 12000*g* for 10 min at 4 ºC to remove any insoluble α-syn aggregates. The supernatant was loaded into a sample loop of the chromatography setup. This sample was then run through Superdex 200 Increase 10/300 GL (GE healthcare, 28990944) column equilibrated with PBS and eluted as 0.5 mL fractions at a flow rate of 0.4 mL/min. The elution of protein was monitored by UV absorbance at 280 nm. The SEC fractions were analyzed by SDS-PAGE analysis, and fractions of interest (oligomer) were collected and stored at 4 ºC.

Preparation of HNE-induced oligomers

HNE-induced oligomers were prepared as described previously (Näsström *et al.* 2011a). Briefly, the recombinant α-syn protein was dissolved in 20 mM Tris and 100 mM NaCl to have a final concentration of 140 µM (pH 7.4). After dissolving, the protein solution was filtered through 100 kDa filter (MERCK, MRCFOR100). The filtrate was transferred to a low-protein binding tube and 30 equivalents of HNE (Cayman Chem, 32100) (final concentration: 4.2mM) was added. This tube was incubated in an incubator at 37ºC under quiescent conditions for 18 hours. Following incubation, the sample was centrifuged at 12000g for 10 min at 4 ºC to remove any insoluble α-syn aggregates. The supernatant was loaded into a sample loop of the chromatography setup. This sample was run through Superdex 200 Increase 10/300 GL (GE healthcare, 28990944) column equilibrated with PBS and eluted as 0.5 mL fractions at a flow rate of 0.4 ml/min. The elution of protein was monitored by UV absorbance at 280nm. The SEC fractions were analyzed by SDS-PAGE analysis, and fractions of interest (oligomer) were collected and stored at 4 ºC.

Protein concentration estimation

The concentration of α-syn samples such as monomers, oligomers, and fibrils were estimated using BCA assay and amino acid analysis. For BCA assay, microplate measurements were carried out using BCA protein assay reagents (Pierce, catalog number: 23227). Briefly, triplicates of known concentrations (from 10 µg/mL-1000 µg/mL) of bovine serum albumin (concentration standard) and an equal volume of α-syn samples were pipetted into microplate wells. To which, 200 µL of BCA working reagent was added and incubated at 37 °C for 30 minutes. Absorbance at 562 nm was measured using a Tecan plate reader. Using BCA assay based concentration estimation as

standards, known concentrations (2-3 µg) of α-syn samples were pipetted into a conical insert, flash-frozen, and lyophilized. The dried form of α-syn samples was shipped to Functional Genomic Center Zurich for subjecting for amino acid analysis (AAA) for absolute quantification of α-syn samples concentrations.

Preparation of WT α-syn fibrils

WT α-syn fibrils were prepared as described in (Mahul-Mellier *et al.* 2020). Briefly, 4 mg of lyophilized recombinant α-syn was dissolved in 50 mM Tris, and 150 mM NaCl and pH was adjusted to 7.5. The solution is filtered through 0.2 µm filters (MERCK, SLGP033RS), and the filtrate is transferred to black screw cap tubes. This tube was incubated in a shaking incubator at 37 ºC and 1000 rpm for five days. After five days, the formation of fibrils was assessed by TEM and SDS-PAGE, followed by Coomassie staining as described in (Mahul-Mellier *et al.* 2018).

Characterization of oligomers

SDS-PAGE analysis

Human WT α-syn monomers, unmodified WT, DA-induced, and HNE-induced oligomers were run on 15% polyacrylamide gels, and Coomassie blue staining was performed as described previously (Kumar *et al.* 2020).

TEM analysis

TEM analysis of protein samples were performed as described previously (Kumar *et al.* 2020). Briefly, 5 µL protein samples were placed on glow discharged Formvar and carbon-coated 200 mesh-containing copper EM grids. After about a minute, the samples were carefully blotted using filter paper and air-dried for 30 s. These grids were washed three times with water and followed by staining with 0.7% (w/v) uranyl formate solution. TEM images were acquired by Tecnai Spirit BioTWIN electron microscope, and image analysis was performed by ImageJ software as described previously (Kumar *et al.* 2020).

Far-UV circular dichroism (CD) spectroscopy

Approximately 150 µL of protein samples were loaded onto 1 mm path length quartz cuvette, and CD spectra were obtained on Chirascan spectropolarimeter (Applied Photophysics) with the

following parameters as described in (Kumar *et al.* 2020). Temperature: 20 ºC; wavelength range: 198 to 250 nm; data pitch: 0.2 nm; bandwidth: 1 nm; scanning speed: 50 nm/min; digital integration time: 2 s. The final CD spectra was a binomial approximation on an average of 10 repeat measurements. The secondary structural content of the oligomers was estimated using the online CD analysis tool known as CAPITO (Wiedemann *et al.* 2013).

Mass spectrometry analysis

Mass spectrometry (MS) analysis of proteins were performed by liquid chromatography-mass spectrometry (LC-MS) on the LTQ system (Thermo Scientific, San Jose, CA). Before analysis, proteins were desalted online by reversed-phase chromatography on a Poroshell 300SB C3 column (1.0x75mm, 5um, Agilent Technologies, Santa Clara, CA, on the LTQ system). 10 uL protein samples were injected on the column at a flow rate of 300 uL/min and were eluted from 5 % to 95 % of solvent B against solvent A, linear gradient. The solvent composition was, Solvent A: 0.1% formic acid in ultra-pure water; solvent B: 0.1% formic acid in acetonitrile. MagTran software (Amgen Inc., Thousand Oaks, CA) was used for charge state deconvolution and MS analysis.

Temperature stability analysis of oligomers

Human WT α-syn unmodified WT, DA-induced and HNE-induced oligomers were tested for their stability at different temperature conditions. Morphological characteristics were assessed by TEM under conditions such as freeze-thaw cycles, storage at 4ºC or 37ºC for 5 days.

Binding characterization of α-syn species to different antibodies

Dot/Slot blot analysis

Nitrocellulose membranes (Amersham, 10600001) were spotted with two different concentrations 12.5 μM and 2.5 μM, corresponding to 180 ng and 36 ng of proteins in duplicates (monomers and oligomers) per sample spot. The membranes were blocked for 1 hour with Odyssey blocking buffer (LiCoR, 927-40000), and then incubated overnight with different primary antibodies (Table 2) diluted in PBST. The membranes were washed three times, with 0.1% PBS-Tween (3x10minutes) and incubated with IRdye conjugated secondary antibodies (1:7500) (Table 1) for 1 hour at RT. Thereafter, the membranes were washed three times, with 0.1% PBS-Tween (3x10minutes). The visualization was performed by fluorescence using Odyssey CLx from LiCor.

Western blot analysis

Approximately 50 ng of proteins (monomers or oligomers) were loaded onto 15 % polyacrylamide gels and run at 180 V for 1 hour. Gels were transferred onto nitrocellulose membranes (Amersham, 10600001) at 25 V, 0.5 A, and 45 minutes using Trans-Blot Turbo (Bio-Rad, 170-4155). The membranes were blocked for 1 hour with Odyssey blocking buffer (LiCoR, 927-40000), and then incubated overnight with different primary antibodies (Table 2) diluted in PBST. The membranes were washed three times, with 0.1% PBS-Tween (3x10minutes) and incubated with IR dye conjugated secondary antibodies (1:7500) (Table 1) for 1 hour at RT. After that, the membranes were washed three times, with 0.1% PBS-Tween (3x10 minutes). The visualization was performed by fluorescence imaging using Odyssey CLx from LiCor.

Determination of antibody affinities by surface plasmon resonance (SPR, BIACORE)

SPR data were collected on a Biacore 8K device (GE Healthcare). Antibodies were immobilized on a CM5 biosensor chip (GE Healthcare) at 10-20 µg/mL concentration in 10 mM acetate solution (GE Healthcare) at pH 4.5 to reach a final surface ligand density of around 2000-4000 response units (RUs). In short, the whole immobilization procedure using solutions of 1-ethyl-3-(3-dimethyl aminopropyl) carbodiimide (EDC) and N-hydroxy succinimide (NHS) mixture, antibody sample and ethanolamine, was carried out at a flow rate of 10 µl/min into the flow cells of the Biacore chip. Firstly, the carboxyl groups on the sensorchip surface were activated by injecting 200 µL of 1:1 (v/v) mixture of EDC/NHS (included in the amine coupling kit, Cytiva life sciences) into both flow cells 1 and 2 and followed by the injection of antibodies overflow cell 2 for 180 s. The remaining activated groups in both the flow cells were blocked by injecting 129 µL of 1 M ethanolamine-HCl pH 8.5. The sensor chip coated with antibodies were equilibrated with PBS buffer before the initiation of the binding assays. Serial dilutions of analytes such as α-syn monomers or oligomers (unmodified oligomers) at a concentration ranging between 2 µM to 0.015 µM in PBS buffer were injected into both flow cells at a flow rate of 30 uL/min at 25 °C. Each sample cycle has the contact time (association phase) of 120 seconds and followed by a dissociation time of 600 seconds. After every injection cycle, surface regeneration of the Biacore chips was performed using 10 mM glycine (pH 3.0). The obtained data were processed and analyzed using Biacore 8K evaluation software for the calculation of the binding kinetics (association rate constant (K_a) and dissociation rate constant (K_d)) and binding affinity (KD). The

fitting of the data was based on either 1:1 binding model (mostly for the monomers) or heterogeneous ligand binding model (for oligomers) using global kinetic fitting unless otherwise noted.

Antibody characterization and stability analysis of oligomers by digital sandwich ELISA using Simoa technology

A sandwich ELISA Simoa immunoassay was used to assess the reactivity of different α-syn antibodies towards α-synuclein forms such as monomers, unmodified oligomers, and fibrils. To prepare the conjugated beads, paramagnetic carboxylated particles/beads were activated for 15 minutes at 4 °C using 0.05 mg/mL of 1-ethyl-3-[3-dimethylaminopropyl]carbodiimide hydrochloride (EDAC) (ThermoScientific, Cat N°A35391) added to $1{,}40\times10^{9}$ beads/mL. The beads were washed using a magnetic separator, and 0.1 mg/mL of the oligomeric α-synuclein specific monoclonal capture antibody was added. After 2 hours of incubation on a mixer-shaker at 4 °C, the conjugation reaction was blocked (Quanterix blocking buffer, Cat N°101356) for 30 minutes at room temperature. The conjugated beads were washed and stored at 4 °C. The biotinylated detector antibody (SYN211) was used with an antibody/biotin ratio of 64. The assay was performed on the fully automated Quanterix Simoa HD-1 with a 2-step protocol. The undiluted samples were tested, which required 300 µL volume of samples without accounting for dead volume (duplicate testing). The calibrator diluent consists of 1xPBS with 0.1% milk, 0.1% Tween. The first incubation step of the sample with the beads was 60 minutes. After washing, the second incubation step with streptavidin-β-galactosidase (Quanterix, Cat N° 103397) was 5 minutes. Prior to reading Resorufin-β-D-galactopyranoside (Quanterix, Cat N° 101736) was added.

References

Arboleda-Velasquez, J. F., Lopera, F., O'Hare, M. et al. (2019) Resistance to autosomal dominant Alzheimer's disease in an APOE3 Christchurch homozygote: a case report. *Nature medicine* **25,** 1680-1683.

Abcam (209538). Anti-Alpha-synuclein filament antibody [MJFR-14-6-4-2] - Conformation-Specific ab209538. Retreived from https://www.abcam.com/alpha-synuclein-filament-antibody-mjfr-14-6-4-2-conformation-specific-ab209538.html

Baba, M., Nakajo, S., Tu, P. H., Tomita, T., Nakaya, K., Lee, V. M., Trojanowski, J. Q. and Iwatsubo, T. (1998) Aggregation of alpha-synuclein in Lewy bodies of sporadic Parkinson's disease and dementia with Lewy bodies. *The American journal of pathology* **152,** 879-884.

Bae, E.-J., Ho, D.-H., Park, E., Jung, J. W., Cho, K., Hong, J. H., Lee, H.-J., Kim, K. P. and Lee, S.-J. (2013) Lipid peroxidation product 4-hydroxy-2-nonenal promotes seeding-capable oligomer formation and cell-to-cell transfer of α-synuclein. *Antioxid Redox Signal* **18,** 770-783.

Broersen, K., van den Brink, D., Fraser, G., Goedert, M. and Davletov, B. (2006) Alpha-synuclein adopts an alpha-helical conformation in the presence of polyunsaturated fatty acids to hinder micelle formation. *Biochemistry* **45,** 15610-15616.

Cappai, R., Leck, S. L., Tew, D. J. et al. (2005) Dopamine promotes alpha-synuclein aggregation into SDS-resistant soluble oligomers via a distinct folding pathway. *FASEB journal : official publication of the Federation of American Societies for Experimental Biology* **19,** 1377-1379.

Cariulo, C., Martufi, P., Verani, M. et al. (2019) Phospho-S129 Alpha-Synuclein Is Present in Human Plasma but Not in Cerebrospinal Fluid as Determined by an Ultrasensitive Immunoassay. *Front Neurosci* **13,** 889-889.

Choi, B.-K., Choi, M.-G., Kim, J.-Y., Yang, Y., Lai, Y., Kweon, D.-H., Lee, N. K. and Shin, Y.-K. (2013) Large α-synuclein oligomers inhibit neuronal SNARE-mediated vesicle docking. *Proceedings of the National Academy of Sciences* **110,** 4087-4092.

Cole, N. B., Murphy, D. D., Lebowitz, J., Di Noto, L., Levine, R. L. and Nussbaum, R. L. (2005) Metal-catalyzed oxidation of alpha-synuclein: helping to define the relationship between oligomers, protofibrils, and filaments. *The Journal of biological chemistry* **280,** 9678-9690.

Colla, E., Coune, P., Liu, Y., Pletnikova, O., Troncoso, J. C., Iwatsubo, T., Schneider, B. L. and Lee, M. K. (2012) Endoplasmic Reticulum Stress Is Important for the Manifestations of α-Synucleinopathy In Vivo. *The Journal of Neuroscience* **32,** 3306-3320.

Colosimo, C., Hughes, A. J., Kilford, L. and Lees, A. J. (2003) Lewy body cortical involvement may not always predict dementia in Parkinson's disease. *Journal of neurology, neurosurgery, and psychiatry* **74,** 852-856.

Conway, K. A., Lee, S. J., Rochet, J. C., Ding, T. T., Williamson, R. E. and Lansbury, P. T., Jr. (2000) Acceleration of oligomerization, not fibrillization, is a shared property of both alpha-synuclein mutations linked to early-onset Parkinson's disease: implications for pathogenesis and therapy. *Proceedings of the National Academy of Sciences of the United States of America* **97,** 571-576.

Conway, K. A., Rochet, J. C., Bieganski, R. M. and Lansbury, P. T., Jr. (2001) Kinetic stabilization of the alpha-synuclein protofibril by a dopamine-alpha-synuclein adduct. *Science (New York, N.Y.)* **294,** 1346-1349.

Cookson, M. R., Hardy, J. and Lewis, P. A. (2008) Genetic neuropathology of Parkinson's disease. *International journal of clinical and experimental pathology* **1,** 217-231.

Covell, D. J., Robinson, J. L., Akhtar, R. S. et al. (2017) Novel conformation-selective alpha-synuclein antibodies raised against different in vitro fibril forms show distinct patterns of Lewy pathology in Parkinson's disease. *Neuropathology and applied neurobiology* **43,** 604-620.

Cremades, N., Chen, S. W. and Dobson, C. M. (2017) Structural Characteristics of alpha-Synuclein Oligomers. *International review of cell and molecular biology* **329,** 79-143.

Cuervo, A. M., Stefanis, L., Fredenburg, R., Lansbury, P. T. and Sulzer, D. (2004) Impaired degradation of mutant alpha-synuclein by chaperone-mediated autophagy. *Science (New York, N.Y.)* **305,** 1292-1295.

Danzer, K. M., Haasen, D., Karow, A. R., Moussaud, S., Habeck, M., Giese, A., Kretzschmar, H., Hengerer, B. and Kostka, M. (2007) Different species of alpha-synuclein oligomers induce calcium influx and seeding. *The Journal of neuroscience : the official journal of the Society for Neuroscience* **27,** 9220-9232.

Danzer, K. M., Kranich, L. R., Ruf, W. P., Cagsal-Getkin, O., Winslow, A. R., Zhu, L., Vanderburg, C. R. and McLean, P. J. (2012) Exosomal cell-to-cell transmission of alpha synuclein oligomers. *Molecular neurodegeneration* **7,** 42.

Danzer, K. M., Krebs, S. K., Wolff, M., Birk, G. and Hengerer, B. (2009) Seeding induced by α-synuclein oligomers provides evidence for spreading of α-synuclein pathology. *Journal of neurochemistry* **111,** 192-203.

De Franceschi, G., Frare, E., Pivato, M., Relini, A., Penco, A., Greggio, E., Bubacco, L., Fontana, A. and de Laureto, P. P. (2011) Structural and morphological characterization of aggregated species of alpha-synuclein induced by docosahexaenoic acid. *The Journal of biological chemistry* **286,** 22262-22274.

Desplats, P., Lee, H. J., Bae, E. J., Patrick, C., Rockenstein, E., Crews, L., Spencer, B., Masliah, E. and Lee, S. J. (2009) Inclusion formation and neuronal cell death through neuron-to-neuron transmission of alpha-synuclein. *Proceedings of the National Academy of Sciences of the United States of America* **106,** 13010-13015.

Di Maio, R., Barrett, P. J., Hoffman, E. K. et al. (2016) alpha-Synuclein binds to TOM20 and inhibits mitochondrial protein import in Parkinson's disease. *Science translational medicine* **8,** 342ra378.

Diógenes, M. J., Dias, R. B., Rombo, D. M. et al. (2012) Extracellular Alpha-Synuclein Oligomers Modulate Synaptic Transmission and Impair LTP Via NMDA-Receptor Activation. *The Journal of Neuroscience* **32,** 11750-11762.

Duffy, P. E. and Tennyson, V. M. (1965) Phase and Electron Microscopic Observations of Lewy Bodies and Melanin Granules in the Substantia Nigra and Locus Caeruleus in Parkinson's Disease*†. *Journal of Neuropathology & Experimental Neurology* **24,** 398-414.

Ehrnhoefer, D. E., Bieschke, J., Boeddrich, A., Herbst, M., Masino, L., Lurz, R., Engemann, S., Pastore, A. and Wanker, E. E. (2008) EGCG redirects amyloidogenic polypeptides into unstructured, off-pathway oligomers. *Nature structural & molecular biology* **15,** 558-566.

El-Agnaf, O. M., Salem, S. A., Paleologou, K. E., Curran, M. D., Gibson, M. J., Court, J. A., Schlossmacher, M. G. and Allsop, D. (2006) Detection of oligomeric forms of alpha-synuclein protein in human plasma as a potential biomarker for Parkinson's disease. *FASEB journal : official publication of the Federation of American Societies for Experimental Biology* **20,** 419-425.

Elfarrash, S., Jensen, N. M., Ferreira, N. et al. (2019) Organotypic slice culture model demonstrates inter-neuronal spreading of alpha-synuclein aggregates. *Acta Neuropathologica Communications* **7,** 213.

Fauvet, B., Mbefo, M. K., Fares, M. B. et al. (2012) alpha-Synuclein in central nervous system and from erythrocytes, mammalian cells, and Escherichia coli exists predominantly as disordered monomer. *The Journal of biological chemistry* **287,** 15345-15364.

Fecchio, C., De Franceschi, G., Relini, A., Greggio, E., Dalla Serra, M., Bubacco, L. and Polverino de Laureto, P. (2013) α-Synuclein Oligomers Induced by Docosahexaenoic Acid Affect Membrane Integrity. *PloS one* **8,** e82732.

Frigerio, R., Fujishiro, H., Ahn, T. B. et al. (2011) Incidental Lewy body disease: do some cases represent a preclinical stage of dementia with Lewy bodies? *Neurobiology of aging* **32,** 857-863.

Gaig, C., Ezquerra, M., Marti, M. J., Muñoz, E., Valldeoriola, F. and Tolosa, E. (2006) LRRK2 Mutations in Spanish Patients With Parkinson Disease: Frequency, Clinical Features, and Incomplete Penetrance. *Archives of Neurology* **63,** 377-382.

Giasson, B. I., Jakes, R., Goedert, M., Duda, J. E., Leight, S., Trojanowski, J. Q. and Lee, V. M. (2000) A panel of epitope-specific antibodies detects protein domains distributed throughout human alpha-synuclein in Lewy bodies of Parkinson's disease. *Journal of neuroscience research* **59,** 528-533.

Goedert, M., Jakes, R. and Spillantini, M. G. (2017) The Synucleinopathies: Twenty Years On. *Journal of Parkinson's disease* **7,** S51-S69.

Guerrero-Ferreira, R., Taylor, N. M., Arteni, A.-A. et al. (2019) Two new polymorphic structures of human full-length alpha-synuclein fibrils solved by cryo-electron microscopy. *Elife* **8,** e48907.

Guo, J. L., Covell, D. J., Daniels, J. P. et al. (2013) Distinct α-synuclein strains differentially promote tau inclusions in neurons. *Cell* **154,** 103-117.

Hamm-Alvarez, S. F., Okamoto, C. T., Janga, S. R. et al. (2019) Oligomeric α-synuclein is increased in basal tears of Parkinson’s patients. *Biomarkers in Medicine* **13,** 941-952.

Hirohata, M., Ono, K., Morinaga, A., Ikeda, T. and Yamada, M. (2011) Cerebrospinal fluid from patients with multiple system atrophy promotes in vitro alpha-synuclein fibril formation. *Neuroscience letters* **491,** 48-52.

Illes-Toth, E., Ramos, M. R., Cappai, R., Dalton, C. and Smith, D. P. (2015) Distinct higher-order alpha-synuclein oligomers induce intracellular aggregation. *Biochem J* **468,** 485-493.

Ingelsson, M. (2016) Alpha-Synuclein Oligomers-Neurotoxic Molecules in Parkinson's Disease and Other Lewy Body Disorders. *Front Neurosci* **10,** 408-408.

Jang, A., Lee, H. J., Suk, J. E., Jung, J. W., Kim, K. P. and Lee, S. J. (2010) Non-classical exocytosis of alpha-synuclein is sensitive to folding states and promoted under stress conditions. *Journal of neurochemistry* **113,** 1263-1274.

Johansen, K. K., Torp, S. H., Farrer, M. J., Gustavsson, E. K. and Aasly, J. O. (2018) A Case of Parkinson's Disease with No Lewy Body Pathology due to a Homozygous Exon Deletion in Parkin. *Case reports in neurological medicine* **2018,** 6838965.

Jung, Y., Whitwell, J. L., Duffy, J. R., Strand, E. A., Machulda, M. M., Senjem, M. L., Jack, C. R., Lowe, V. J. and Josephs, K. A. (2016) Regional beta-amyloid burden does not correlate with cognitive or language deficits in Alzheimer's disease presenting as aphasia. *European journal of neurology* **23,** 313-319.

Kaufmann, T. J., Harrison, P. M., Richardson, M. J., Pinheiro, T. J. and Wall, M. J. (2016) Intracellular soluble alpha-synuclein oligomers reduce pyramidal cell excitability. *The Journal of physiology* **594,** 2751-2772.

Kawahata, I., Bousset, L., Melki, R. and Fukunaga, K. (2019) Fatty Acid-Binding Protein 3 is Critical for α-Synuclein Uptake and MPP(+)-Induced Mitochondrial Dysfunction in Cultured Dopaminergic Neurons. *Int J Mol Sci* **20,** 5358.

Kay, D. M., Kramer, P., Higgins, D., Zabetian, C. P. and Payami, H. (2005) Escaping Parkinson's disease: a neurologically healthy octogenarian with the LRRK2 G2019S mutation. *Movement disorders : official journal of the Movement Disorder Society* **20,** 1077-1078.

Klucken, J., Poehler, A. M., Ebrahimi-Fakhari, D. et al. (2012) Alpha-synuclein aggregation involves a bafilomycin A 1-sensitive autophagy pathway. *Autophagy* **8,** 754-766.

Kovacs, G. G., Wagner, U., Dumont, B. et al. (2012) An antibody with high reactivity for disease-associated alpha-synuclein reveals extensive brain pathology. *Acta neuropathologica* **124,** 37-50.

Kumar, S. T., Donzelli, S., Chiki, A., Syed, M. M. K. and Lashuel, H. A. (2020) A simple, versatile and robust centrifugation-based filtration protocol for the isolation and quantification of alpha-synuclein monomers, oligomers and fibrils: Towards improving experimental reproducibility in alpha-synuclein research. *Journal of neurochemistry* **153,** 103-119.

Lashuel, H. A. (2020) Do Lewy bodies contain alpha-synuclein fibrils? and Does it matter? A brief history and critical analysis of recent reports. *Neurobiology of disease***,** 104876.

Lashuel, H. A. and Lansbury, P. T. (2006) Are amyloid diseases caused by protein aggregates that mimic bacterial pore-forming toxins? *Quarterly Reviews of Biophysics* **39,** 167-201.

Lashuel, H. A., Petre, B. M., Wall, J., Simon, M., Nowak, R. J., Walz, T. and Lansbury, P. T., Jr. (2002) Alpha-synuclein, especially the Parkinson's disease-associated mutants, forms pore-like annular and tubular protofibrils. *Journal of molecular biology* **322,** 1089-1102.

Lassen, L. B., Gregersen, E., Isager, A. K., Betzer, C., Kofoed, R. H. and Jensen, P. H. (2018) ELISA method to detect α-synuclein oligomers in cell and animal models. *PloS one* **13,** e0196056.

Lee, H. J., Suk, J. E., Bae, E. J., Lee, J. H., Paik, S. R. and Lee, S. J. (2008) Assembly-dependent endocytosis and clearance of extracellular alpha-synuclein. *The international journal of biochemistry & cell biology* **40,** 1835-1849.

Leong, S. L., Cappai, R., Barnham, K. J. and Pham, C. L. (2009) Modulation of alpha-synuclein aggregation by dopamine: a review. *Neurochemical research* **34,** 1838-1846.

Li, B., Ge, P., Murray, K. A. et al. (2018) Cryo-EM of full-length α-synuclein reveals fibril polymorphs with a common structural kernel. *Nature Communications* **9,** 3609.

Lowe, R., Pountney, D. L., Jensen, P. H., Gai, W. P. and Voelcker, N. H. (2004) Calcium(II) selectively induces alpha-synuclein annular oligomers via interaction with the C-terminal domain. *Protein science : a publication of the Protein Society* **13,** 3245-3252.

Mahul-Mellier, A.-L., Altay, M. F., Burtscher, J. et al. (2018) The making of a Lewy body: the role of α-synuclein post-fibrillization modifications in regulating the formation and the maturation of pathological inclusions. *bioRxiv***,** 500058.

Mahul-Mellier, A.-L., Burtscher, J., Maharjan, N., Weerens, L., Croisier, M., Kuttler, F., Leleu, M., Knott, G. W. and Lashuel, H. A. (2020) The process of Lewy body formation, rather than simply α-synuclein fibrillization, is one of the major drivers of neurodegeneration. *Proceedings of the National Academy of Sciences* **117,** 4971-4982.

Mahul-Mellier, A. L., Vercruysse, F., Maco, B., Ait-Bouziad, N., De Roo, M., Muller, D. and Lashuel, H. A. (2015) Fibril growth and seeding capacity play key roles in alpha-synuclein-mediated apoptotic cell death. *Cell death and differentiation* **22,** 2107-2122.

Majbour, N. K., Vaikath, N. N., van Dijk, K. D. et al. (2016) Oligomeric and phosphorylated alpha-synuclein as potential CSF biomarkers for Parkinson's disease. *Molecular neurodegeneration* **11,** 7.

Martinez, T. N., Jensen, P. H., Luk, K.C. et al. (2016) The Michael J. Fox Foundation's Strategy to Generate, Characterize, and Distribute Preclinical Alpha-Synuclein Research Tools for Molecular Biology. MJFF poster **413.21**. https://files.michaeljfox.org/TNM_asyn_molecular_tools_poster_2016.pdf

Mor, D. E., Tsika, E., Mazzulli, J. R. et al. (2017) Dopamine induces soluble alpha-synuclein oligomers and nigrostriatal degeneration. *Nature neuroscience* **20,** 1560-1568.

Näsström, T., Fagerqvist, T., Barbu, M. et al. (2011a) The lipid peroxidation products 4-oxo-2-nonenal and 4-hydroxy-2-nonenal promote the formation of α-synuclein oligomers with distinct biochemical, morphological, and functional properties. *Free radical biology & medicine* **50,** 428-437.

Näsström, T., Gonçalves, S., Sahlin, C., Nordström, E., Screpanti Sundquist, V., Lannfelt, L., Bergström, J., Outeiro, T. F. and Ingelsson, M. (2011b) Antibodies against Alpha-Synuclein Reduce Oligomerization in Living Cells. *PloS one* **6,** e27230.

Nasstrom, T., Wahlberg, T., Karlsson, M., Nikolajeff, F., Lannfelt, L., Ingelsson, M. and Bergstrom, J. (2009) The lipid peroxidation metabolite 4-oxo-2-nonenal cross-links alpha-synuclein causing rapid formation of stable oligomers. *Biochemical and biophysical research communications* **378,** 872-876.

Nelson, P. T., Alafuzoff, I., Bigio, E. H. et al. (2012) Correlation of Alzheimer disease neuropathologic changes with cognitive status: a review of the literature. *Journal of neuropathology and experimental neurology* **71,** 362-381.

Norris, E. H., Giasson, B. I., Hodara, R., Xu, S., Trojanowski, J. Q., Ischiropoulos, H. and Lee, V. M. (2005) Reversible inhibition of alpha-synuclein fibrillization by dopaminochrome-mediated conformational alterations. *The Journal of biological chemistry* **280,** 21212-21219.

Paleologou, K. E., Kragh, C. L., Mann, D. M. A., Salem, S. A., Al-Shami, R., Allsop, D., Hassan, A. H., Jensen, P. H. and El-Agnaf, O. M. A. (2009) Detection of elevated levels of soluble α-synuclein oligomers in post-mortem brain extracts from patients with dementia with Lewy bodies. *Brain* **132,** 1093-1101.

Parihar, M. S., Parihar, A., Fujita, M., Hashimoto, M. and Ghafourifar, P. (2009) Alpha-synuclein overexpression and aggregation exacerbates impairment of mitochondrial functions by augmenting oxidative stress in human neuroblastoma cells. *The international journal of biochemistry & cell biology* **41,** 2015-2024.

Parkkinen, L., Kauppinen, T., Pirttila, T., Autere, J. M. and Alafuzoff, I. (2005) Alpha-synuclein pathology does not predict extrapyramidal symptoms or dementia. *Annals of neurology* **57,** 82-91.

Parkkinen, L., Pirttila, T. and Alafuzoff, I. (2008) Applicability of current staging/categorization of alpha-synuclein pathology and their clinical relevance. *Acta neuropathologica* **115,** 399-407.

Paslawski, W., Andreasen, M., Nielsen, S. B., Lorenzen, N., Thomsen, K., Kaspersen, J. D., Pedersen, J. S. and Otzen, D. E. (2014a) High stability and cooperative unfolding of alpha-synuclein oligomers. *Biochemistry* **53,** 6252-6263.

Paslawski, W., Lorenzen, N. and Otzen, D. E. (2016) Formation and Characterization of alpha-Synuclein Oligomers. *Methods in molecular biology (Clifton, N.J.)* **1345,** 133-150.

Paslawski, W., Mysling, S., Thomsen, K., Jørgensen, T. J. D. and Otzen, D. E. (2014b) Co-existence of Two Different α-Synuclein Oligomers with Different Core Structures Determined by Hydrogen/Deuterium Exchange Mass Spectrometry. *Angewandte Chemie International Edition* **53,** 7560-7563.

Perrin, R. J., Payton, J. E., Barnett, D. H., Wraight, C. L., Woods, W. S., Ye, L. and George, J. M. (2003) Epitope mapping and specificity of the anti-alpha-synuclein monoclonal antibody Syn-1 in mouse brain and cultured cell lines. *Neuroscience letters* **349,** 133-135.

Planchard, M. S., Exley, S. E., Morgan, S. E. and Rangachari, V. (2014) Dopamine-induced alpha-synuclein oligomers show self- and cross-propagation properties. *Protein science : a publication of the Protein Society* **23,** 1369-1379.

Polymeropoulos, M. H., Lavedan, C., Leroy, E. et al. (1997) Mutation in the alpha-synuclein gene identified in families with Parkinson's disease. *Science (New York, N.Y.)* **276,** 2045-2047.

Qin, Z., Hu, D., Han, S., Reaney, S. H., Di Monte, D. A. and Fink, A. L. (2007) Effect of 4-hydroxy-2-nonenal modification on alpha-synuclein aggregation. *The Journal of biological chemistry* **282,** 5862-5870.

Rekas, A., Knott, R. B., Sokolova, A. et al. (2010) The structure of dopamine induced alpha-synuclein oligomers. *European biophysics journal : EBJ* **39,** 1407-1419.

Roberts, R. F., Wade-Martins, R. and Alegre-Abarrategui, J. (2015) Direct visualization of alpha-synuclein oligomers reveals previously undetected pathology in Parkinson's disease brain. *Brain* **138,** 1642-1657.

Rockenstein, E., Nuber, S., Overk, C. R. et al. (2014) Accumulation of oligomer-prone alpha-synuclein exacerbates synaptic and neuronal degeneration in vivo. *Brain* **137,** 1496-1513.

Ruesink, H., Reimer, L., Gregersen, E., Moeller, A., Betzer, C. and Jensen, P. H. (2019) Stabilization of α-synuclein oligomers using formaldehyde. *PloS one* **14,** e0216764.

Ruggeri, F. S., Benedetti, F., Knowles, T. P. J., Lashuel, H. A., Sekatskii, S. and Dietler, G. (2018) Identification and nanomechanical characterization of the fundamental single-strand protofilaments of amyloid α-synuclein fibrils. *Proceedings of the National Academy of Sciences* **115,** 7230-7235.

Sampson, T. R., Debelius, J. W., Thron, T. et al. (2016) Gut Microbiota Regulate Motor Deficits and Neuroinflammation in a Model of Parkinson's Disease. *Cell* **167,** 1469-1480 e1412.

Schmidt, F., Levin, J., Kamp, F., Kretzschmar, H., Giese, A. and Botzel, K. (2012) Single-channel electrophysiology reveals a distinct and uniform pore complex formed by alpha-synuclein oligomers in lipid membranes. *PloS one* **7,** e42545.

Shahmoradian, S. H., Lewis, A. J., Genoud, C. et al. (2019) Lewy pathology in Parkinson's disease consists of crowded organelles and lipid membranes. *Nature neuroscience* **22,** 1099-1109.

Sharon, R., Bar-Joseph, I., Frosch, M. P., Walsh, D. M., Hamilton, J. A. and Selkoe, D. J. (2003) The formation of highly soluble oligomers of alpha-synuclein is regulated by fatty acids and enhanced in Parkinson's disease. *Neuron* **37,** 583-595.

Spillantini, M. G., Crowther, R. A., Jakes, R., Hasegawa, M. and Goedert, M. (1998) alpha-Synuclein in filamentous inclusions of Lewy bodies from Parkinson's disease and dementia with lewy bodies. *Proceedings of the National Academy of Sciences of the United States of America* **95,** 6469-6473.

Spillantini, M. G., Schmidt, M. L., Lee, V. M., Trojanowski, J. Q., Jakes, R. and Goedert, M. (1997) Alpha-synuclein in Lewy bodies. *Nature* **388,** 839-840.

Stöckl, M. T., Zijlstra, N. and Subramaniam, V. (2013) α-Synuclein Oligomers: an Amyloid Pore? *Molecular Neurobiology* **47,** 613-621.

Tekirdag, K. and Cuervo, A. M. (2018) Chaperone-mediated autophagy and endosomal microautophagy: Joint by a chaperone. *The Journal of biological chemistry* **293,** 5414-5424.

Tofaris, G. K., Razzaq, A., Ghetti, B., Lilley, K. S. and Spillantini, M. G. (2003) Ubiquitination of alpha-synuclein in Lewy bodies is a pathological event not associated with impairment of proteasome function. *The Journal of biological chemistry* **278,** 44405-44411.

Tokuda, T., Qureshi, M. M., Ardah, M. T. et al. (2010) Detection of elevated levels of alpha-synuclein oligomers in CSF from patients with Parkinson disease. *Neurology* **75,** 1766-1772.

Trostchansky, A., Lind, S., Hodara, R., Oe, T., Blair, I. A., Ischiropoulos, H., Rubbo, H. and Souza, J. M. (2006) Interaction with phospholipids modulates alpha-synuclein nitration and lipid-protein adduct formation. *Biochem J* **393,** 343-349.

Tsigelny, I. F., Sharikov, Y., Miller, M. A. and Masliah, E. (2008) Mechanism of alpha-synuclein oligomerization and membrane interaction: theoretical approach to unstructured proteins studies. *Nanomedicine* **4,** 350-357.

Vaikath, N. N., Majbour, N. K., Paleologou, K. E. et al. (2015) Generation and characterization of novel conformation-specific monoclonal antibodies for alpha-synuclein pathology. *Neurobiology of disease* **79,** 81-99.

van Diggelen, F., Hrle, D., Apetri, M., Christiansen, G., Rammes, G., Tepper, A. and Otzen, D. E. (2019) Two conformationally distinct α-synuclein oligomers share common epitopes and the ability to impair long-term potentiation. *PloS one* **14,** e0213663.

Vivacqua, G., Latorre, A., Suppa, A. et al. (2016) Abnormal Salivary Total and Oligomeric Alpha-Synuclein in Parkinson's Disease. *PloS one* **11,** e0151156.

Volles, M. J., Lee, S. J., Rochet, J. C., Shtilerman, M. D., Ding, T. T., Kessler, J. C. and Lansbury, P. T., Jr. (2001) Vesicle permeabilization by protofibrillar alpha-synuclein: implications for the pathogenesis and treatment of Parkinson's disease. *Biochemistry* **40,** 7812-7819.

Volpicelli-Daley, L. A., Luk, K. C., Patel, T. P., Tanik, S. A., Riddle, D. M., Stieber, A., Meaney, D. F., Trojanowski, J. Q. and Lee, V. M. (2011) Exogenous alpha-synuclein fibrils induce Lewy body pathology leading to synaptic dysfunction and neuron death. *Neuron* **72,** 57-71.

Wang, W., Perovic, I., Chittuluru, J. et al. (2011) A soluble α-synuclein construct forms a dynamic tetramer. *Proceedings of the National Academy of Sciences* **108,** 17797-17802.

Weihofen, A., Liu, Y., Arndt, J. W. et al. (2019) Development of an aggregate-selective, human-derived α-synuclein antibody BIIB054 that ameliorates disease phenotypes in Parkinson's disease models. *Neurobiology of disease* **124,** 276-288.

Wiedemann, C., Bellstedt, P. and Görlach, M. (2013) CAPITO--a web server-based analysis and plotting tool for circular dichroism data. *Bioinformatics (Oxford, England)* **29,** 1750-1757.

Wilms, H., Rosenstiel, P., Romero-Ramos, M. et al. (2009) Suppression of MAP kinases inhibits microglial activation and attenuates neuronal cell death induced by alpha-synuclein protofibrils. *International journal of immunopathology and pharmacology* **22,** 897-909.

Wright, J. A., Wang, X. and Brown, D. R. (2009) Unique copper-induced oligomers mediate alpha-synuclein toxicity. *The FASEB Journal* **23,** 2384-2393.

Xiang, W., Schlachetzki, J. C., Helling, S. et al. (2013) Oxidative stress-induced posttranslational modifications of alpha-synuclein: specific modification of alpha-synuclein by 4-hydroxy-2-nonenal increases dopaminergic toxicity. *Molecular and cellular neurosciences* **54,** 71-83.

Figure legends

Figure 1: A schematic illustration of our antibody validation strategy. In brief, the pipeline included the preparation of well-defined preparations of α-syn monomers, oligomers, and fibrils. Oligomers were generated from three different protocols to capture the morphological and structural heterogeneity. The α-syn conformation-specific antibodies were procured from different sources. The reactivity of these antibodies was assessed using slot blot, Western blot, and a digital sandwich ELISA (SIMOA) assays and SPR studies for selected antibodies to determine the binding affinity and kinetics.

Figure 2: Preparation and characterization of α-syn monomers, oligomers, and fibrils. (A) A scheme depicting the preparation of α-syn monomers, oligomers, and fibrils. (B) SEC purification of monomers and unmodified oligomers. (C and D) SDS-PAGE analysis followed by Coomassie staining of unmodified oligomers (C) and monomers (D) purified from B. (E) ESI-MS spectra of monomers separated by SEC. (F) Comparison of the CD spectra of monomers and oligomers. Oligomers were predominantly enriched in β-sheet structures and monomers showed a predominantly disordered structure. (G) Negatively stained EM analysis performed on monomers. (H) Negatively stained EM analysis performed on unmodified oligomers. (I) Width distribution of unmodified oligomers. (J) CD spectra of fibrils. (K) SDS-PAGE analysis followed by Coomassie staining of the total, supernatant, and pellet fractions obtained during fibril preparation. The pellet fraction is the fibril fraction devoid of monomers and oligomers that was used for further binding studies. (L) Negatively stained EM analysis performed on fibrils. (M) Width distribution of the fibrils. (N) EM images of unmodified oligomers subjected to different temperature conditions, such as freeze-thawing and incubation at 4 °C and 37 °C and (O) the width distribution. P and Q**)** Two concentrations of unmodified oligomers (20 pg/mL (P) and 100 pg/mL (Q)) were incubated at three different temperatures (4°C, 22°C and 37°C) for varying times (2 h, 4 h and 24 h) and with different numbers of freeze-thaw (F/T) cycles (1x, 3x, and 5x) (X-axis). The obtained signals (AEB) from the immunoassay with the antibody A17183B were plotted on the Y-axis. The dashed lines represent the reference condition "ref" and a 10% decrease/increase in the AEB signal as arbitrary thresholds.

Figure 3: *In vitro* binding analysis of antibodies against α-syn monomers, unmodified oligomers and fibrils using slot blots and Western blots, and binding kinetics as determined by SPR. (A) Slot blot analysis to study the reactivity of antibodies against monomers, unmodified oligomers and fibrils under native conditions, spotted with two different concentrations 12.5 μM and 2.5 μM, corresponding to 180 ng and 36 ng of α-syn in duplicates per sample spot. Antibodies clones (5G4, A17183E, and SYNO3) binding with higher specificity to oligomers and fibrils. Antibodies clones (7015, 9029, 12C6, MJFR-14, SYN211, MJFR-14, and SYN-1) that bound to monomers, oligomers and fibrils nonspecifically compared to clones 24H6, A17183A, 26F1, 26B10, A17183G, SYNO2, A17183B, and SYNO4, which showed weak reactivity toward monomers at low concentrations but showed relatively higher reactivity toward oligomers and fibrils. (B) Western blot analysis to study the reactivity of antibodies under denaturing conditions. Antibodies clones (5G4, 24H6, and A17183A) that showed little or no reactivity toward monomers, oligomers, and high molecular weight bands in fibrils. Antibodies clones (A17183E, 26F1) that detected monomers weakly but detected oligomers and high molecular weight bands in fibrils. Antibodies clones (SYN03, A17183B, SYN211, MJFR-14, SYN-1, 26B10, 9029, 12C6, and MFR-14) that strongly detected monomers, oligomers, and high molecular weight bands in fibrils. Abbreviations: M: Monomers; UO: Unmodified Oligomers; F: Fibrils

Figure 4: ELISA Simoa assay of antibodies against monomers, unmodified oligomers and fibrils. The 15 α-synuclein conformation specific antibodies were coupled to the beads as capture monoclonal antibodies (X-axis). α-synuclein monomers (A), oligomers (B), and fibrils (C) were used as the analyte (100 and 1000 pg/mL).The detector antibody was a C-terminal monoclonal antibody (clone SYN211) with an epitope in the amino acid region from 121-125. The signal-to-noise values (S/N) are indicated on the Y-axis for the three α-syn forms. * indicates the availability of only 100 pg/mL oligomer data for antibody clone 9029 (B).

Figure 5: Preparation of dopamine- and HNE-induced oligomers and their stability analysis. (A) and (B) Chemical structures of dopamine and HNE, respectively. (C) and (D) SEC purification of DA-induced oligomers and HNE-induced oligomers separated from monomers, respectively. (E) CD spectra indicate the disordered structures of DA-induced oligomers. (F) Coomassie staining indicating the presence of dopamine and DA-induced oligomers in the stacking gel. (G) Negatively stained EM analysis performed on DA-induced oligomers. DA-induced oligomers showed mainly spherical, undefined morphologies. (H) DA-induced oligomers subjected to different temperature conditions, such as freeze-thawing and incubation at 4 °C and 37 °C to assess their stability. (I) Comparison of the width distribution of DA-induced oligomers subjected to stability analysis. (J) CD spectra indicating the disordered structures of HNE-induced oligomers. (K) Coomassie staining indicating the presence of HNE-induced oligomers in the stacking gel. (L) Negatively stained EM analysis performed on HNE-induced oligomers. HNE-induced oligomers showed mainly spaghetti-shaped structures. (M) HNE-induced oligomers subjected to different temperature conditions, such as freeze-thawing and incubation at 4 °C, and 37 °C to assess their

stability. (N) Comparison of the width distribution of HNE-induced oligomers subjected to stability analysis.

Figure 6: Slot blot analysis of antibodies against α-syn monomers and DA- and HNE-induced oligomers. (A) Slot blot analysis to study the reactivity of antibodies against DA- oligomers, monomers and HNE- oligomers under native conditions, spotted with two different concentrations 12.5 μM and 2.5 μM, corresponding to 180 ng and 36 ng of α-syn in duplicates per sample spot. Antibody clones (5G4, A17183E, and 24H6) bind more specifically to DA- and HNE-induced oligomers than monomers. Antibody clones (SYNO3, A17183A, 26B10, A17183G, SYNO2, A17183B, SYNO4, 7015, 9029, 12C6, MJFR-14, SYN211, MJFR-14, and SYN-1) bind to monomers and DA- and HNE-induced oligomers nonspecifically. The antibody clone 26F1 detected HNE-induced oligomers more specifically than monomers but failed to detect DA-induced oligomers. Abbreviations: M: Monomers; DO: Dopamine-induced oligomers; HO: HNE-induced oligomers.

Figure 7: SPR-based kinetic analysis of different immobilized monoclonal antibodies (A17183A (B), 12C6 (C), and SYN211 (D)) binding to α-syn monomers (top) and unmodified oligomers (bottom) at 30, 60, 120, 250, 500, 1000 and 2000 nM concentrations. The antibodies were immobilized at a ligand density of approximately 3000-4000 Rus. The α-syn monomers or oligomers were injected for 2 min, followed by 5 min dissociation with injection of PBS buffer at a 30 μL/min flow rate. The sensorgrams are shown as colored lines representing varying concentrations of α-syn monomers or oligomers, and the fits are shown as black lines. The kinetic parameters obtained from the fitting are shown in Table 3.

Figures

Figure 1

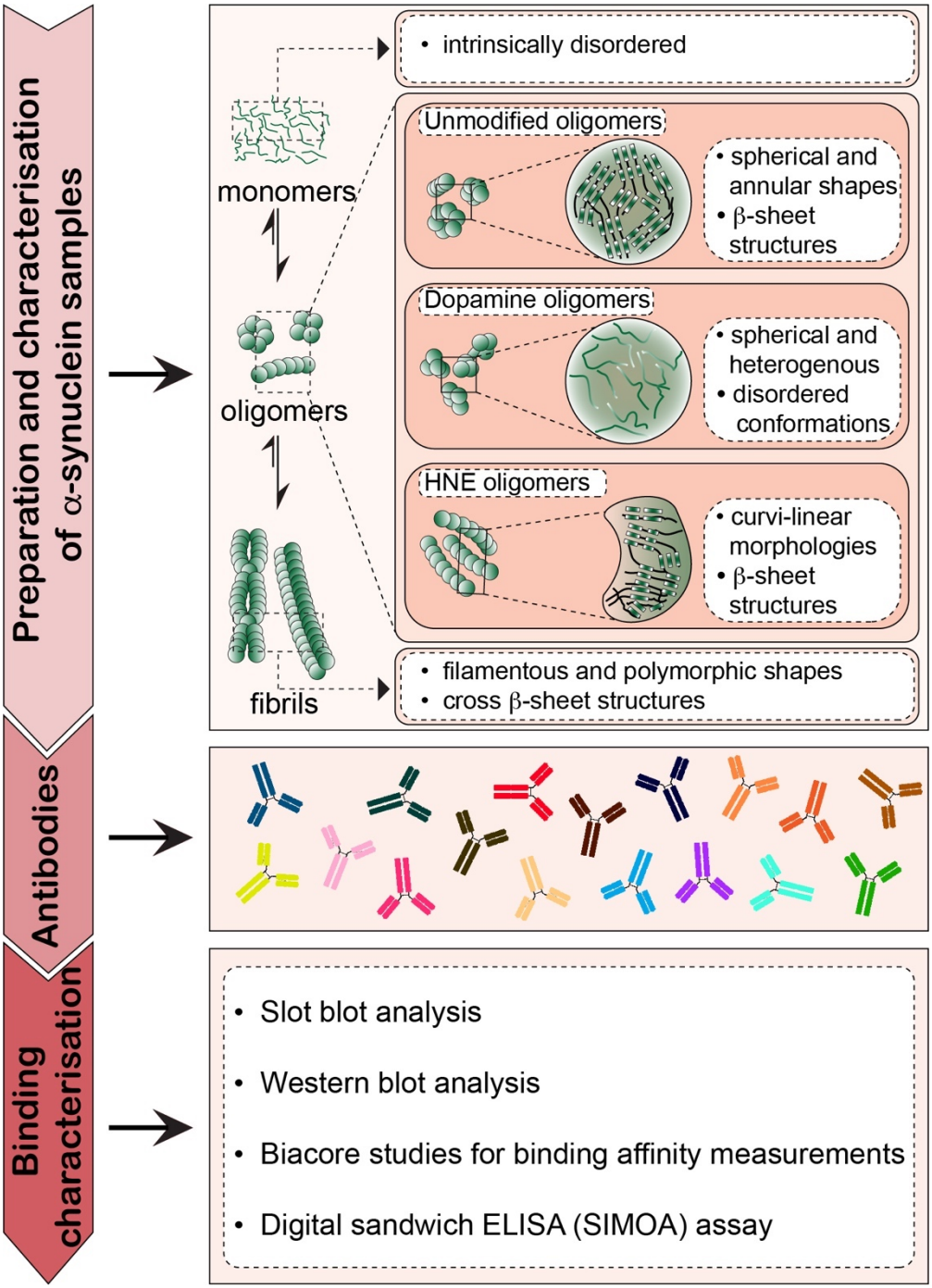

Figure 2

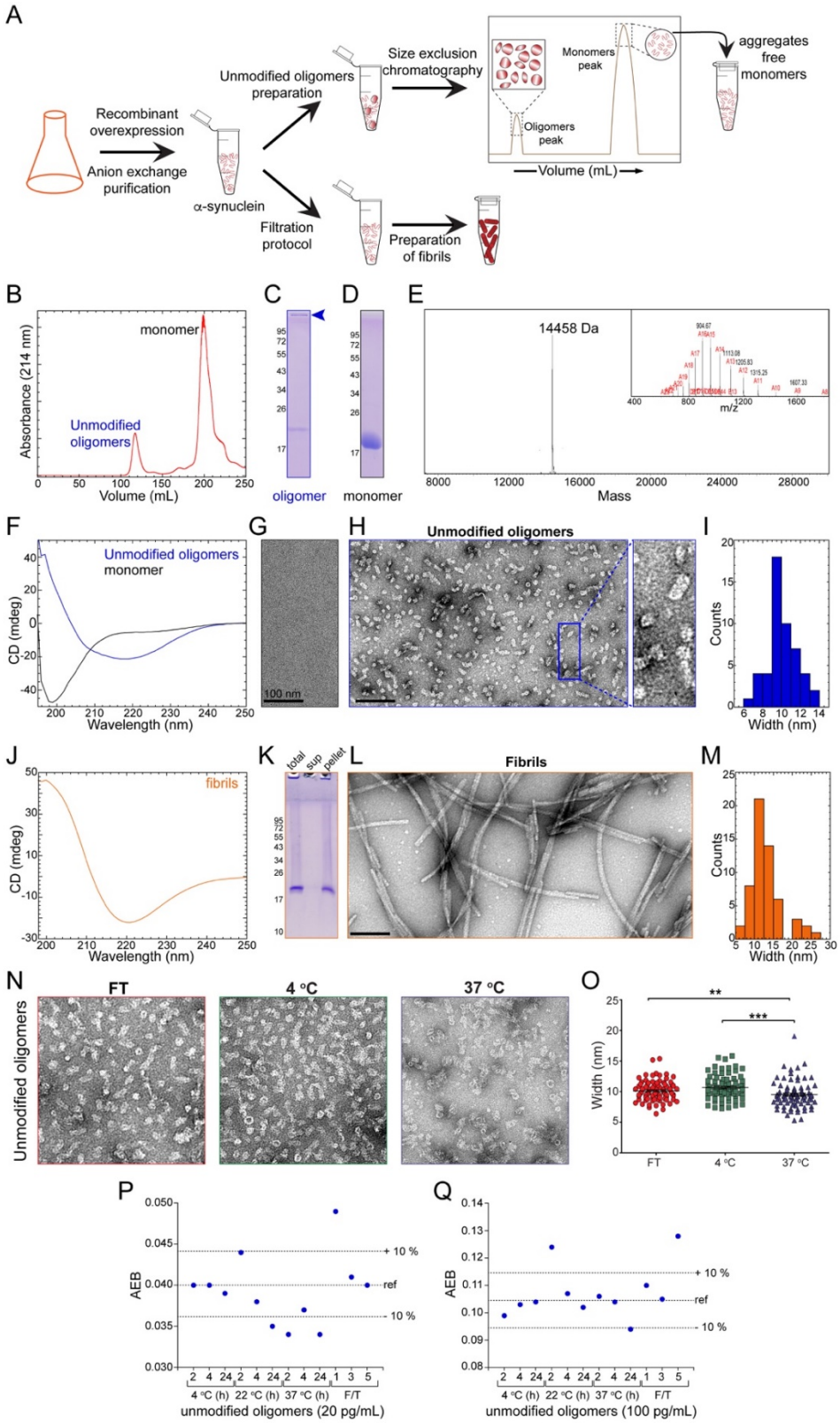
A
Recombinant overexpression
Anion exchange purification
α-synuclein
Unmodified oligomers preparation
Size exclusion chromatography
Monomers peak
Oligomers peak
Volume (mL)
aggregates free monomers
Filtration protocol
Preparation of fibrils
B
Absorbance (214 nm)
monomer
Unmodified oligomers
Volume (mL)
C
oligomer
D
monomer
E
14458 Da
m/z
Mass
F
Unmodified oligomers
monomer
CD (mdeg)
Wavelength (nm)
G
100 nm
H
Unmodified oligomers
I
Counts
Width (nm)
J
fibrils
CD (mdeg)
Wavelength (nm)
K
total
sup
pellet
L
Fibrils
M
Counts
Width (nm)
N
FT
4 °C
37 °C
Unmodified oligomers
O
Width (nm)
FT
4 °C
37 °C
P
AEB
+ 10 %
ref
- 10 %
4 °C (h) 22 °C (h) 37 °C (h) F/T
unmodified oligomers (20 pg/mL)
Q
AEB
+ 10 %
ref
- 10 %
4 °C (h) 22 °C (h) 37 °C (h) F/T
unmodified oligomers (100 pg/mL)

Figure 3

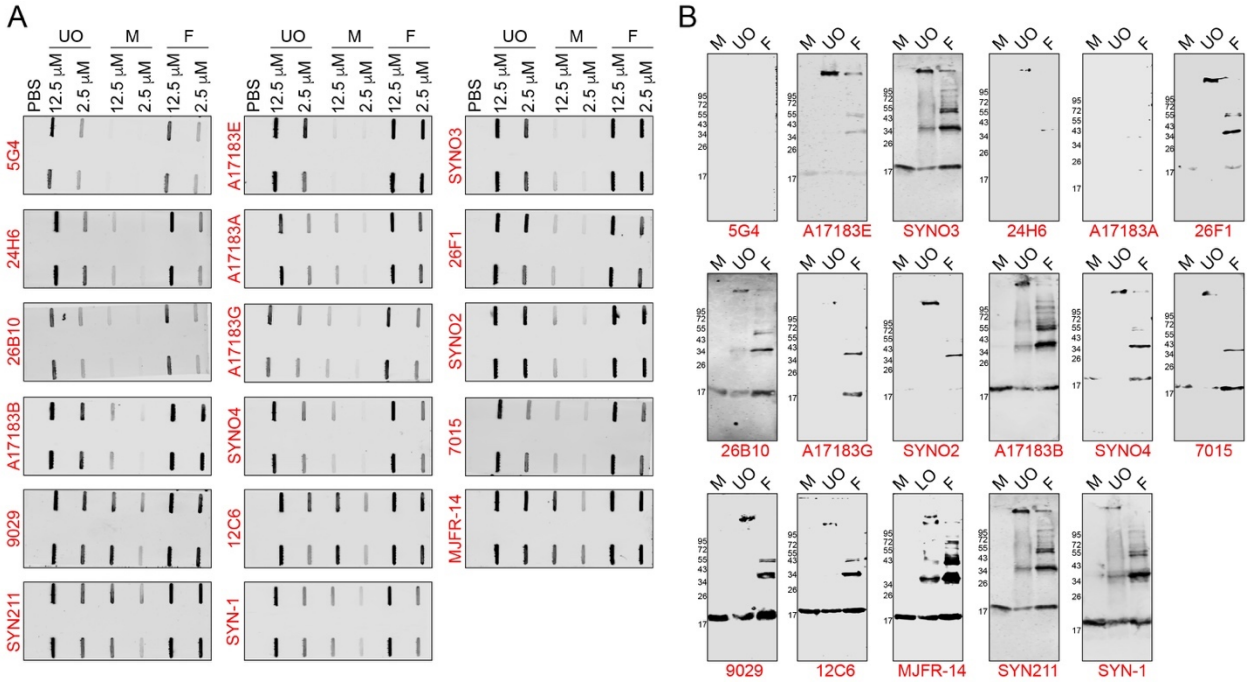

Figure 4

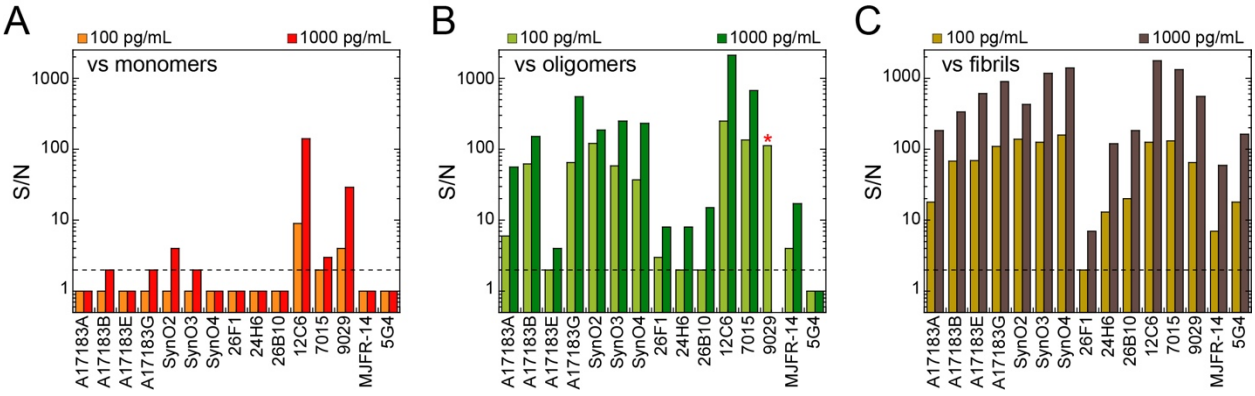

Figure 5

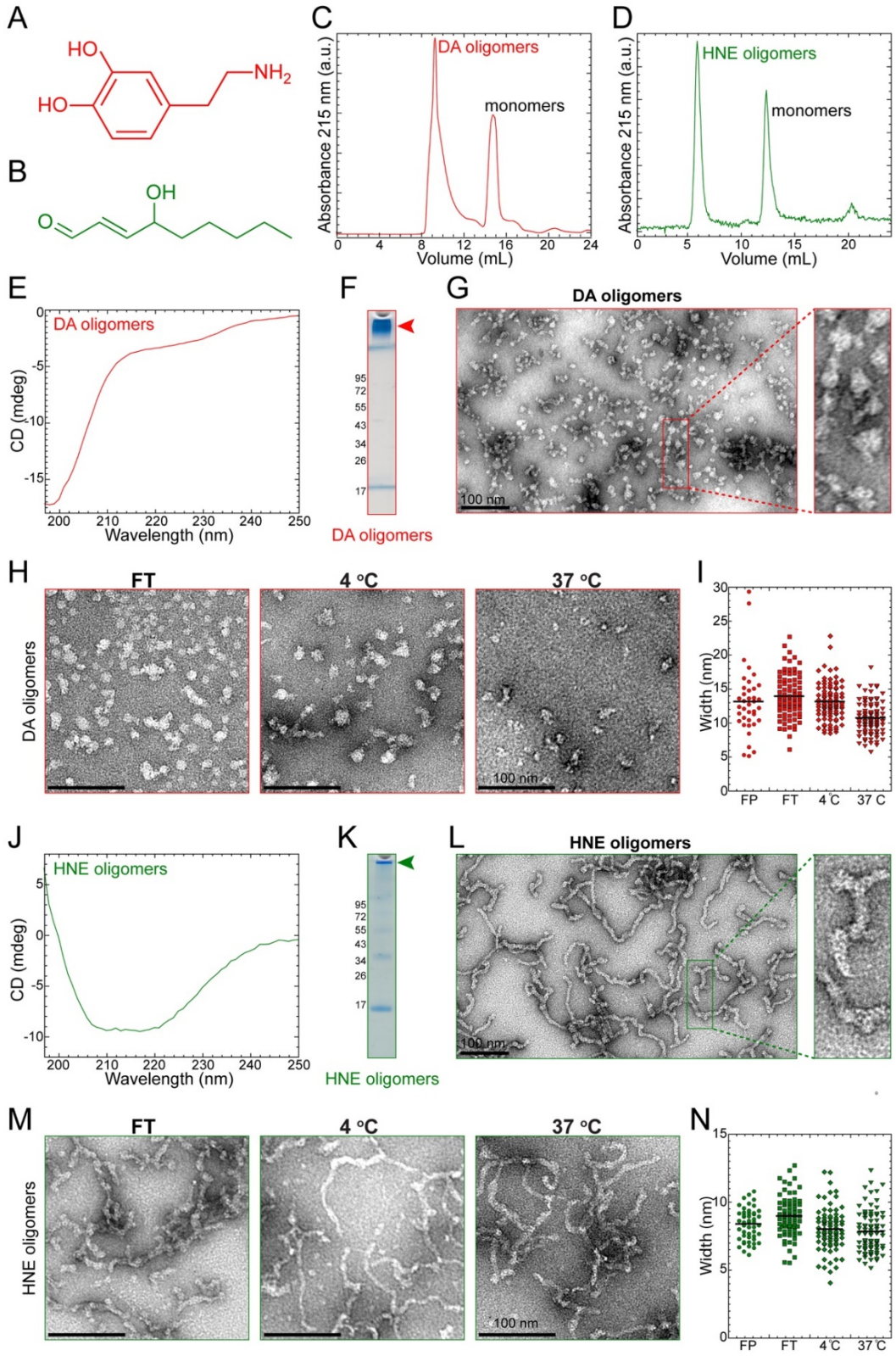
A
HO
HO
NH2
B
OH
O
C
DA oligomers
monomers
Absorbance 215 nm (a.u.)
Volume (mL)
D
HNE oligomers
monomers
Absorbance 215 nm (a.u.)
Volume (mL)
E
DA oligomers
CD (mdeg)
Wavelength (nm)
F
95
72
55
43
34
26
17
DA oligomers
G
DA oligomers
100 nm
H
FT
4 °C
37 °C
DA oligomers
100 nm
I
Width (nm)
FP
FT
4 °C
37 °C
J
HNE oligomers
CD (mdeg)
Wavelength (nm)
K
95
72
55
43
34
26
17
HNE oligomers
L
HNE oligomers
100 nm
M
FT
4 °C
37 °C
HNE oligomers
100 nm
N
Width (nm)
FP
FT
4 °C
37 °C

Figure 6

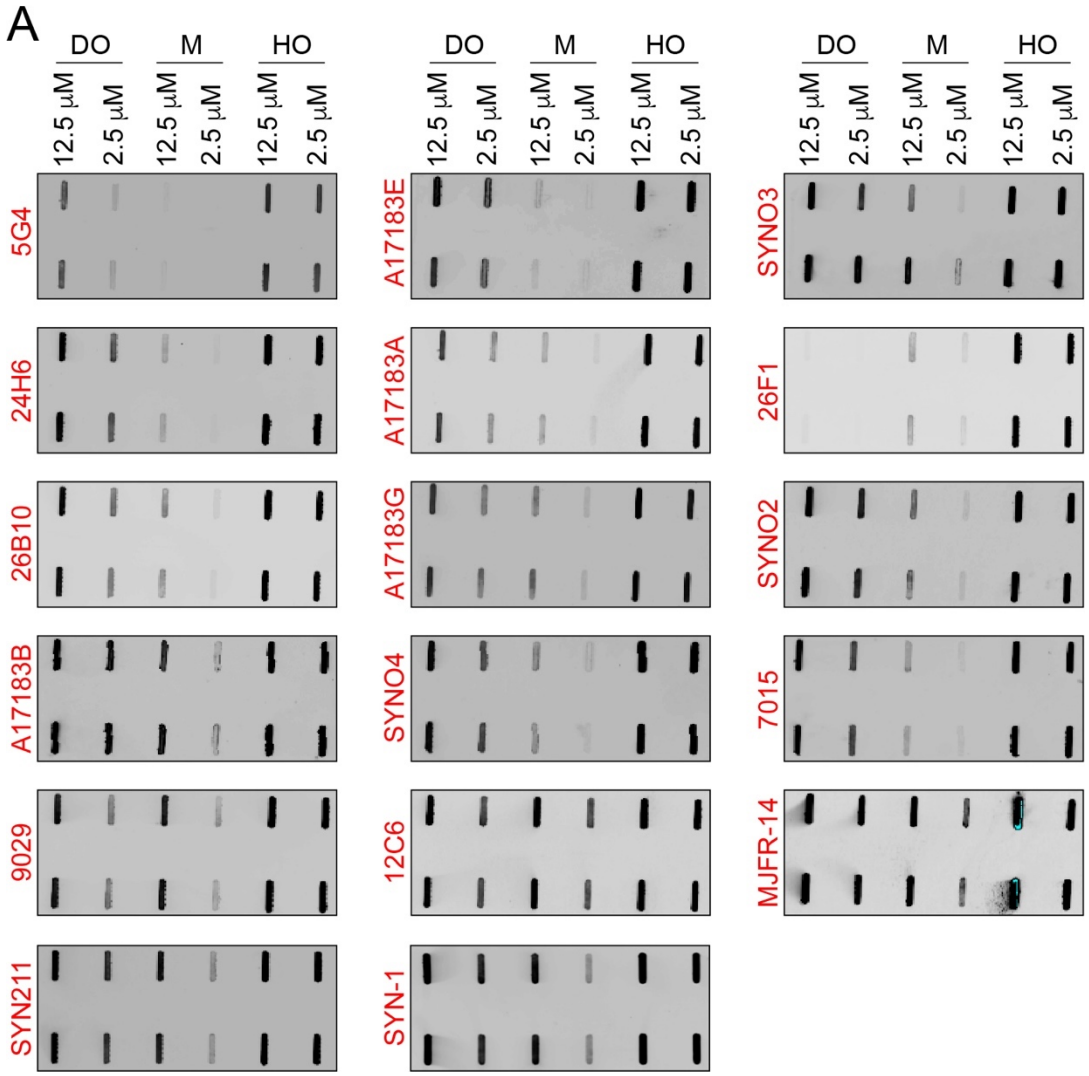
A
DO
M
HO
12.5 μM
2.5 μM
5G4
24H6
26B10
A17183B
9029
SYN211
A17183E
A17183A
A17183G
SYNO4
12C6
SYN-1
SYNO3
26F1
SYNO2
7015
MJFR-14

Figure 7

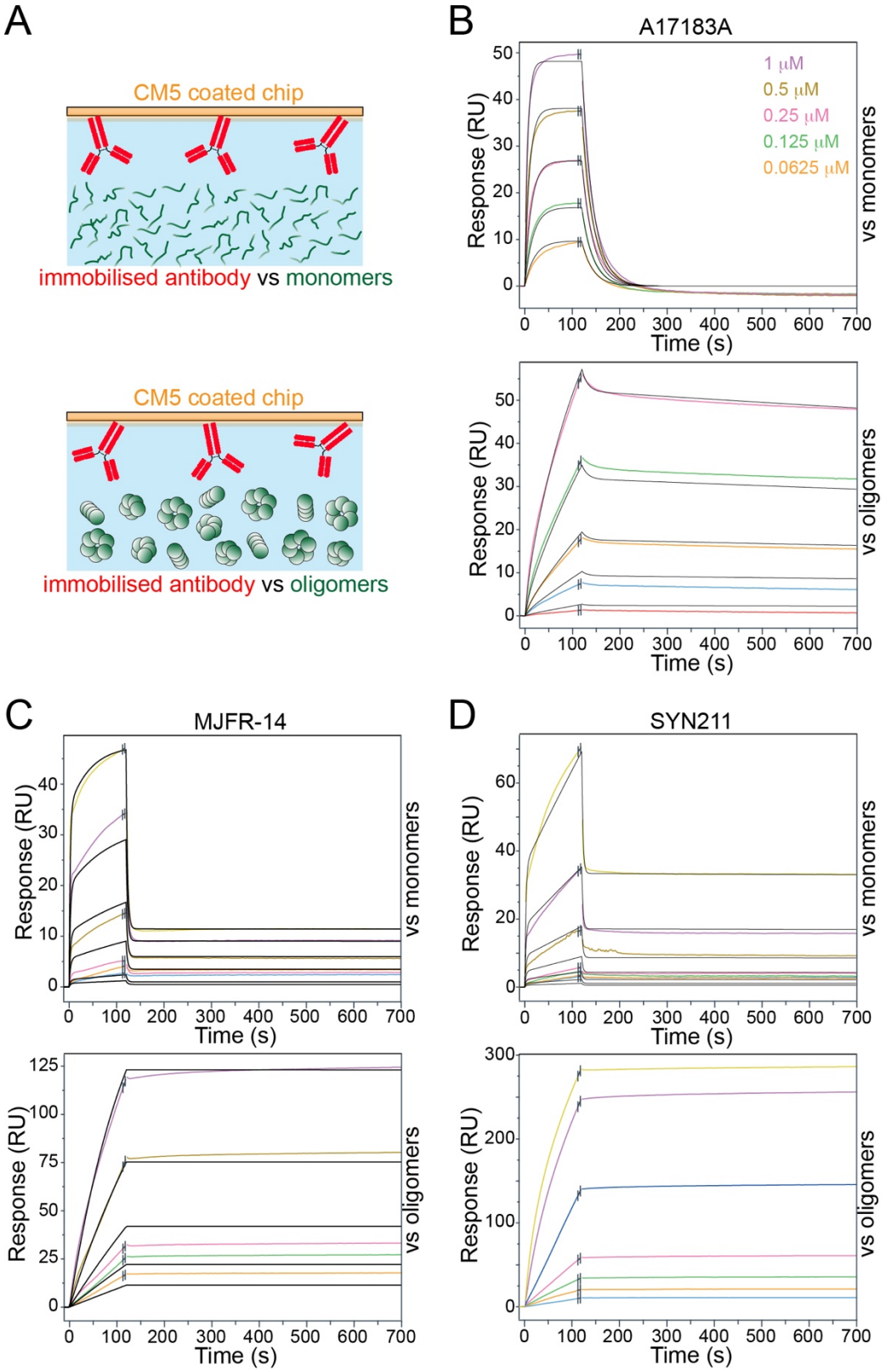
A
CM5 coated chip
immobilised antibody vs monomers
CM5 coated chip
immobilised antibody vs oligomers
B
A17183A
1 μM
0.5 μM
0.25 μM
0.125 μM
0.0625 μM
Response (RU)
Time (s)
vs monomers
vs oligomers
C
MJFR-14
D
SYN211

Tables

Table 1: Materials and Reagents

Equipment/Material description	Supplier	Catalogue/Reference
Chromatography columns		
HiPrep Q FF 16/10	GE healthcare	28936543
Hiload 26/600 superdex 200pg	GE healthcare	28-9893-36
Superdex 200 Increase 10/300 GL	GE healthcare	28990944
Tubes and Filters and dialysis membrane		
Low protein binding tubes	Eppendorf	022431081
30 kDa MWCO	MERCK	UFC903008
100 kDa MWCO	MERCK	MRCFOR100
0.22 um filters	MERCK	SLGP033RS
0.45 um filters	MERCK	SLFH05010
12-14 kDa MWCO dialysis membrane	Spectrum Labs	9.206 67
Chemicals and Reagents		
TRIS	Biosolve	200923
Ampicillin	AppliChem	A0839
IPTG	Biochemica	A1008
EDTA-free Protease Inhibitor Cocktail	SIGMA	11873580001
PMSF	Applichem	A0999
Dopamine	Sigma Aldrich	H8502
4-hydroxy Nonenal (HNE)	Cayman Chem	32100
Benzonase® Nuclease HC	MERCK	71205-3
Centrifuges and Sonicator		
Ultrasonicator	VibraCell, Sonics	VCX130
Benchtop centrifuge	Eppendorf	5417R
Ultracentrifuge	Beckmann Coulter	Optima Max XD
Blocking Buffer and Secondary Antibodies		
Odyssey blocking buffer	LiCoR	927-40000
Goat anti-mouse AF680	Invitrogen	A21058
Goat anti-rabbit AF800	Invitrogen	926-32211
Goat anti-rat IRDye 680RD	LiCoR	P/N 926-68076

Table 2: List and details of antibodies used in this study

Antibody (clones)	Source	Specificity	Immunogen	Epitope	Isotype	Host	Original Reference	Characterization by purified α-syn standards in the original reference
24H6	MJFF DOSAB*	conformational	HNE-induced oligomers	not reactive towards recombinant FL α-syn nor synthetic peptides in the amino acid region 96-140	IgG2a, κ	Mouse monoclonal	(van Diggelen *et al.* 2019)#	NA
26B10					IgG2a, κ			
26F1					IgG2a, κ			
12C6			DHA induced oligomers	reacts with synthetic peptide in the amino acid region 113-140	IgG2a, κ			
7015	UPenn	conformational	Strain A, *in vitro* α-syn PFF	recognizes a discontinuous epitope with binding elements in the extreme C-terminus and near amino acid 50	NA	Mouse monoclonal	(Covell *et al.* 2017) (Guo *et al.* 2013)	Yes, Sandwich ELISA using Strain A fibrils, Strain B fibrils and monomer
9029			Strain B, *in vitro* α-syn PFF	amino acids 32 – 58				
SYNO2	Biolegend	conformational	α-syn fibrils (50 µg/mouse)	Weak signal for amino acids 127-140 detected by ELISA	IgG1	Mouse monoclonal	(Vaikath *et al.* 2015)	Yes, dot blot, inhibition ELISA, sandwich ELISA using fibrils and monomers
SYNO3					IgG1			
SYNO4					IgG1			
A17183A	Biolegend	conformational	Recombinant α-syn aggregate	NA	IgG2a, κ	Rat monoclonal	BioLegend Cat. No. 864901	NA
A17183E					NA		NA	
A17183G					IgG1, κ		BioLegend Cat. No. 865103	
A17183B					IgG2a, κ		BioLegend Cat. No. 865001	
MJFR-14	MJFF/Abcam	conformational	Recombinant α-syn filament amino acids 1 to the C-term	NA	NA	Rabbit monoclonal	Martinez et al., 2016, Poster 413.21 Abcam Cat. No. ab209538	Yes, dot blot using filament, oligomer and monomer Luminex assay using monomer, oligomer and fibrils
5G4	Kovacs (Merck millipore)	Aggregated α-syn	TKEGVVHGVATV AE (44 – 57)	amino acids 46 – 53	IgG1, κ	Mouse monoclonal	(Kovacs *et al.* 2012)	No
SYN211	Abcam	Non-conformational	Recombinant full-length Human α-syn	amino acids 121 – 125	IgG1	Mouse monoclonal	(Giasson *et al.* 2000), Abcam Cat. No. ab80627	Yes, WB using monomer
SYN-1	BD-biosciences	Non-conformational	Rat Synuclein-1 amino acids 15-123	amino acids 91 – 99	IgG1	Mouse monoclonal	(Perrin *et al.* 2003) BD-biosciences Cat. No. 610787	Yes, WB using monomer

*Antibodies were generated by ADx NeuroSciences in a MJFF sponsored project (DOSAB) in collaboration with Crossbeta.

Reference contains the information of the immunogen used for the generation of antibodies.

DHA: docosahexaenoic acid; NA: informations not available

Table 3: Kinetic parameters of the antibodies binding to α-syn monomers or oligomers

Immobillised antibodies	Injected α-syn	$k_a(M^{-1}s^{-1})$	$k_d(s^{-1})$	KD
A17183A	monomers	1.18×10^4	4.26×10^{-2}	3.61 μM
	oligomers	K_{a1}:2.31×10^4 K_{a2}:2.99×10^3	K_{d1}:8.46×10^{-2} K_{d2}:1.35×10^{-4}	KD1: 3.67 μM KD2: 45 nM
SYNO4	monomers	1.22×10^4	6.93×10^{-2}	5.67 μM
	oligomers	K_{a1}:4.25×10^5 K_{a2}:2.34×10^4	K_{d1}:1.06×10^{-1} K_{d2}:5.01×10^{-7}	KD1: 249 nM KD2: 2.14 pM
26F1	monomers	2.58×10^2	1.97×10^{-2}	76 μM
	oligomers	K_{a1}:1.01×10^4 K_{a2}:7.94×10^3	K_{d1}:2.13×10^{-2} K_{d2}:2.22×10^{-6}	KD1: 2.12 μM KD2: 279 pM
12C6	monomers	K_{a1}:5.87×10^4 K_{a2}:4.60×10^4	K_{d1}:4.32×10^{-2} K_{d2}:3.86×10^{-3}	KD1: 737 nM KD2: 8.4 nM
	oligomers	K_{a1}:4.43×10^7 K_{a2}:1.32×10^4	K_{d1}:3.29×10^{-1} K_{d2}:9.83×10^{-6}	KD1: 7.4 nM KD2: 0.74 nM
MJFR-14	monomers	K_{a1}:1.04×10^5 K_{a2}:2.22×10^4	K_{d1}:3.43×10^{-1} K_{d2}:5.7×10^{-6}	KD1: 3.29 μM KD2: 0.25 nM
	oligomers	K_{a1}:9.07×10^5 K_{a2}:1.54×10^4	K_{d1}:6.95×10^{-4} K_{d2}:4.31×10^{-7}	KD1: 0.76 nM KD2: 2.8 pM
9029	monomers	No fitting	No fitting	No fitting
	oligomers	No fitting	No fitting	No fitting
SYN211	monomers	K_{a1}:1.52×10^4 K_{a2}:8.37×10^2	K_{d1}:4.10×10^{-1} K_{d2}:1.81×10^{-5}	KD1: 271 μM KD2: 217 nM
	oligomers	No fitting	No fitting	No fitting

Table 4: Morphologies and structural properties of oligomers used in this study

Oligomers	Morphologies	Width/diameter	Secondary structure composition (%)		
			α-helix	β-strand	irregular
Unmodified oligomers	annular pore, spherical, tubular	6-14 nm	27	38	32
DA oligomers	near-spherical, globular	5-20 nm	11	11	78
HNE oligomers	curvi-linear	5-11 nm	27	26	49

Table 5: Reactivity and binding specificity of antibodies by different techniques

Category based on type of Immunogen	Antibodies	Dot blot analysis					Western blot analysis◆			ELISA assay			SPR	
		M	UO	DO	HO	F	M	UO	F	M	UO	F	M	UO
Oligomer	26F1#	+	+++	--	+++	+++	--	+++	+	--	++	++	*	***
	12C6	+++	+++	+++	+++	+++	+++	+++	+++	+++	+++	+++	***	***
	24H6	+	+++	+++	+++	+++	--	+	--	+	++	+++	-	-
	26B10	+	++	+++	+++	++	++	++	+++	+	++	+++	-	-
Fibrils	7015	+	+++	+++	+++	+++	+	+	+	++	+++	+++	-	-
	9029	+++	+++	+++	+++	+++	+++	+++	+++	+++	+++	+++	***	***
	SYNO2	+	+++	+++	+++	+++	--	+++	+	+	+++	+++	-	-
	SYNO3	+	+++	+++	+++	+++	+++	+++	+++	+	+++	+++	-	-
	SYNO4#	+	+++	+++	+++	+++	+	+++	+	--	+++	+++	*	***
recombinant α-syn aggregate	A17183A	+	+++	+++	+++	+++	--	--	--	--	+++	+++	*	***
	A171183B	+	+++	+++	+++	+++	+++	+++	+++	+	+++	+++	-	-
	A17183E	--	+++	+++	+++	+++	--	+++	+	+	++	+++	-	-
	A17183G	+	++	+++	+++	+++	--	--	+	+	+++	+++	-	-
a.a. (44-57)	5G4	--	+++	++	+++	++	--	--	--	+	+	+++	-	-
a.a. (1-140)	SYN211	+++	+++	+++	+++	+++	+++	+++	+++	-	-	-	***	***
a.a. (15-123)	SYN-1	+++	+++	+++	+++	+++	+++	+++	+++	-	-	-	-	-
α-syn from 1- the C-term	MJFR-14	+++	+++	+++	+++	+++	+++	+++	+++	--	+++	+++	***	***

M: monomers; UO: unmodified oligomers; DO: DA induced oligomers; HO: HNE induced oligomers; F: fibrils.
-- : no detection; + : faint detection; ++ : medium detection; +++ : strong detection; - : not available
*** : Strong Affinity; * : Weak affinity
◆# for Western blot analysis, detection mentioned is for monomeric α-syn bands (for 26F1 and SYNO4, detection was seen with HMW α-syn bands but not to monomeric bands)